Titre: Title:	Conducted electromagnetic interference mitigation using active filtering method in DC/DC converters
Auteur: Author:	Djilali Hamza
Date:	2006
Type:	Mémoire ou thèse / Dissertation or Thesis
Référence: Citation:	Hamza, D. (2006). Conducted electromagnetic interference mitigation using active filtering method in DC/DC converters [Master's thesis, École Polytechnique de Montréal]. PolyPublie. https://publications.polymtl.ca/7841/

URL de PolyPublie: PolyPublie URL:	https://publications.polymtl.ca/7841/
Directeurs de recherche: Advisors:	Mohamad Sawan
Programme: Program:	Unspecified

UNIVERSITÉ DE MONTRÉAL

CONDUCTED ELECTROMAGNETIC INTERFERENCE MITIGATION USING ACTIVE FILTERING METHOD IN DC/DC CONVERTERS

DJILALI HAMZA

DÉPARTEMENT DE GÉNIE ÉLECTRIQUE

ÉCOLE POLYTECHNIQUE DE MONTRÉAL

MÉMOIRE PRÉSENTÉ EN VUE DE L'OBSTENTION

DU DILÔME DE MAÎTRISE ÉS SCIENCES APPLIQUÉES

(GÉNIE ÉLECTRIQUE)

DÉCEMBRE 2006

Your file Votre référence
ISBN: 978-0-494-25545-2
Our file Notre référence
ISBN: 978-0-494-25545-2

UNIVERSITÉ DE MONTRÉAL

ÉCOLE POLYTECHNIQUE DE MONTRÉAL

Ce mémoire intitulé:

CONDUCTED ELECTROMAGNETIC INTERFERENCE MITIGATION USING ACTIVE FILTERING METHOD IN DC/DC CONVERTERS

Présenté par: DJILALI, Hamza

En vue de l'obtention du diplôme de : Maîtrise ès sciences appliquées

a été dûment acceptée par le jury d'examen constitué de :

M. Abdelhakim Khouas, Ph.D., président

M. Mohamad Sawan, Ph.D., directeur de recherche

M. Gouchuan Zhou, Ph.D., membre du jury

ACKNOWLEDGMENTS

I wish to express my sincere gratitude to my supervisor Dr. Mohamad Sawan in giving me a chance to work on this subject in an excellent condition. I also, wish to thank him for his support and encouragement during the course of this milestone.

I thank my wife Mei for her patience and understandings.

To my daughter Myriam and my son Yusuf

RÉSUMÉ

La réduction du bruit électromagnétique est un sujet très important qui doit être examiné dans la première phase de la conception d'un convertisseur DC/DC qui utilise une fréquence de découpage pour garder une puissance de sortie constante. Ce type de convertisseurs est connu d'être la source des interférences électromagnétiques, principalement due à l'action du circuit du découpage mené par un transistor MOSFET. Le bruit qui existe entre la borne positive et le châssis est désigné comme bruit en mode commun. Ce type de bruit forme la majorité des émissions conductibles. Une partie du bruit en mode commun est convertie en un bruit différentiel qui est généré entre la borne positive et son retour (borne négative).

Pour répondre aux exigences de la compatibilité électromagnétique (CEM) en terme d'émissions de bruit conductibles, les filtres passifs LC ont été toujours une solution intuitive pour réduire le bruit d'interférence électromagnétique (IEM). On peut les trouver presque dans tous les convertisseurs DC/DC à fréquence de découpage. Par contre, leurs dimensions, poids et coûts peuvent engendrer des contraintes dans certaines applications.

Ce projet vise a réalisé une méthode différente de filtrage du bruit pour surmonter les contraintes de la méthode du filtrage passive. Un filtre IEM actif est proposé dans ce

projet. Ce filtre actif utilise l'image du bruit de courant, déphasée par 180 degrés et injectée à la borne positive du convertisseur DC/DC. La combinaison du filtre IEM actif avec le filtre passif a montré une réduction substantielle des émissions de bruit électromagnétique conductibles, comparé a celle d'un filtre passif uniquement. Cette combinaison a non seulement réduit le bruit IEM mais aussi la géométrie et le poids du filtre passif incorporé dans le convertisseur.

Les résultats expérimentaux présentés dans ce mémoire démontrent la performance et l'efficacité du filtre IEM actif recherché dans un convertisseur DC/DC à fréquence de découpage.

ABSTRACT

Electromagnetic interference has been always a concern in electronic systems, in particular at the point of the power supply. It is known that DC/DC converters are the principle culprits in generating conducted noise interference due to the switching action of their MOSFET which is the main element of the DC to DC conversion that use Pulse Width Modulation techniques (PWM) to step-up or to step-down the input voltage to the desired output level. Passive filters have been a straightforward solution to overcome typical conducted electromagnetic interference (EMI) problems at the expense of space, weight and power losses that can be reflected in the final product. The objective of this project is to find an EMI filtering method which does not depend on the input parameters of the power supply such as current and voltage which have direct effect on the size and the weight of the product.

To overcome these constraints, an active EMI filter is proposed. The active EMI filter is based on the image of the noise current phase shifted by 180 degrees and injected back to the DC bus to cancel out the incident noise. However, the combination of the active and the passive filters shows a substantial attenuation of the conducted EMI emissions as compared to the passive filter only. Also, this combination contributes to an important reduction of the size and weight of the passive filter. A complete circuit including the DC/DC converter has been designed and tested. Experimental results to demonstrate the performance and the effectiveness of the active EMI filter in DC/DC converters are presented.

CONDENSÉ EN FRANCAIS

L'évolution des convertisseurs DC/DC a suivit un parcourt très remarquable, vis-à-vis de leur densité de puissance par centimètre carrée et leur dissipation thermique très basse. Cette évolution est due principalement à l'augmentation de leur fréquence de découpage qui a abouti sur un changement rapide du courant instantané di/dt et de la tension dv/dt. Cela engendre une quantité considérable de bruits électromagnétiques. La plupart de ces convertisseurs sont installés sur un circuit imprimé à proximité d'un microprocesseur pour lui fournir une tension de ravitaillement en DC. Donc, avoir un convertisseur DC/DC qui cohabite avec un microprocesseur sans aucune perturbation opérationnelle, représente un défit dans la conception du convertisseur. On défini la compatibilité électromagnétique (CEM) par le processus d'avoir un système, sous système, ou un circuit électronique, qui fonctionne comme il a été conçu dans un environnement électromagnétique sans perturber les autres équipements et sans être perturbé par celles-ci. La CEM est une partie intégrale d'un projet de conception et doit être adressée à la phase initiale du projet.

1. Introduction

Le bruit électromagnétique existe en mode rayonné dans l'air (champs électromagnétique) ou en mode conduit dans une ligne de transmission tel que un câble d'alimentation ou les pistes d'un circuit imprimé. Ces perturbations se propagent par le biais de phénomènes de couplage: un câble peut rayonner un champ électromagnétique et

inversement un champ peut induire un courant parasite sur un conducteur. Cependant, dans ce projet juste les perturbations en mode conduit seront concernées. Les émissions conductibles se divisent en deux modes de bruit, le bruit en mode commun qui est le bruit qui circule entre la borne positive et la borne négative, et le bruit en mode différentiel qui circule entre la borne positive et la mass. Ces deux modes de bruits peuvent être atténués en connectant une haute impédance en série tel qu'une inductance dont l'impédance augmente proportionnellement avec la fréquence du bruit, cette impédance en série empêche le passage du bruit vers l'entrée du convertisseur. Une autre impédance en parallèle tel qu'un condensateur, est placée à l'entrée du convertisseur pour dévier le bruit vers la mise de terre, puisque l'impédance aux bornes d'un condensateur est inversement proportionnelle à la fréquence du bruit. Cette méthode de filtration du bruit est appelée une filtration passive, puisque des éléments passifs L et C sont utilisés. Il est important d'estimer la valeur du bruit en mode commun et celle du mode différentielle dans un convertisseur pour une conception adéquate du filtre passive.

L'application des normes de la CEM et leurs limites, dépend du domaine et l'environnement dans lequel le convertisseur sera installé. Dans certains cas, un seul étage ne suffit pas pour réduire le bruit en dessous des limites des normes de la CEM, on ajoute parfois plusieurs étages pour abaisser le bruit au delà des limites. Cependant, cette solution augmente les dimensions et les pertes thermiques du convertisseur qui ne sont pas permises dans certaines applications. Comme solution alternative, une combinaison d'un filtre actif et un filtre passif LC (un seul étage), d'où le nom hybride, sera proposé

pour aboutir à une réduction optimale du bruit conductible. L'avantage de cette combinaison, c'est d'avoir moins de composants, de petites dimensions, un poids léger et une faible dissipation thermique. L'intégration de cette combinaison de filtres dans un convertisseur DC/DC devrait permettre au convertisseur de se conformer aux normes de la CEM. La figure CF.1 montre les possibilités de placements de la combinaison du filtre actif/passif dans un convertisseur DC/DC. Soit à l'entrée du convertisseur ou bien à sa sortie.

A ce jour, il y a quelques travaux qui ont été réalisés dans ce domaine, en utilisant un filtre actif à la sortie d'un convertisseur [6]-[7]. Le problème avec cette approche c'est que l'inductance du filtre, connecté à la sortie du convertisseur, doit subir le courant de sortie maximal, ce qui exige une grande dimension de l'inductance ce qui n'est pas toujours faisable. En plus, tous ces travaux sont centrés sur l'atténuation du bruit en mode différentielle, au lieu du bruit en mode commun qui représente la partie dominante du bruit total conductible dans le convertisseur. Dans ce projet, les efforts ont été accordés pour explorer la combinaison de deux filtres actif et passif en ce qui concerne l'atténuation du bruit en mode commun à l'entrée du convertisseur. Dans ce cas, l'inductance du filtre passif va subir un courant deux ou trois fois moins que le courant de sortie, ce qui est traduit par une petite dimension de l'inductance. En plus, en utilisant la combinaison à l'entrée du convertisseur, elle devient indépendante de la topologie du convertisseur et ne risque pas d'interférer avec sa boucle de contrôle. Les étapes de cette recherche se détaillent comme suit :

La section 2 présente la description et l'analyse du filtre hybride. La section 3 illustre les paramètres à considérer et la conception du filtre hybride proposé. La section 4 décrit les résultats expérimentaux et les tests réalisés sur le convertisseur DC/DC avec le filtre hybride actif et passif et sans le filtre actif. Une comparaison a été donnée pour montrer les performances des deux configurations. Finalement, une conclusion est déduite de cette recherche.

Erreur ! Liaison incorrecte.

Figure CF. 1 Deux possibilités de placement de la combinaison hydride de filtre, (a) Filtration du bruit à l'entrée du convertisseur; (b) Filtration du bruit à la sortie du convertisseur

2. Description et analyse du filtre actif

2.1 Description du circuit

La configuration du filtre hybride comprend un filtre passif et un filtre actif comme indiqué sur la figure CF.2. L_{in} et C_{in} sont des éléments du filtre passive. Le filtre actif

comprend plusieurs éléments, dont un circuit de détection R_sC_s, un circuit opamp (actif) et un transformateur d'injection du signal.

Le bruit en mode commun du courant, qui circule à l'entrée du convertisseur, est détecté par la branche R_sC_s qui est un filtre passe-haut. Ce type de détecteur est simple et efficace qui bloque tout signal continu, en laissant passer le bruit au delà de certaines fréquences de coupure. Le signal détecté est appliqué à un opamp inverseur pour une inversion du signal d'entrée. A la sortie de l'opamp, on obtient un signal du bruit identique en amplitude et déphasé de 180 degrés par rapport au signal d'entrée. Ce signal est injecté dans la borne positive à l'entrée du convertisseur, à travers un transformateur à haute fréquence (HF) pour atténuer le bruit incident. Ce principe est fondé sur la superposition de deux signaux de même amplitude et de phase opposée.

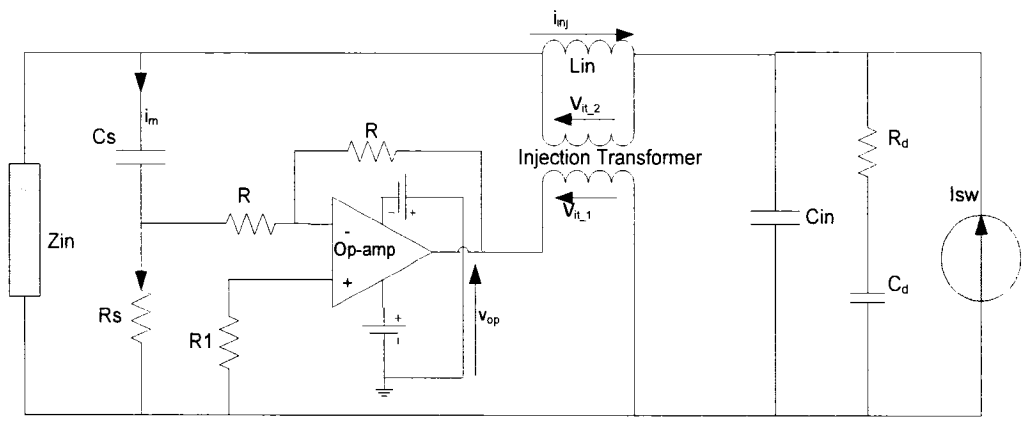

Figure CF. 2 La configuration du filtre hybride proposé

2.2 Analyse du circuit

Considérons un convertisseur DC/DC avec une source d'impédance Z_{in} et une source de bruit d'un courant I_n engendré par la fréquence de commutation. Le schéma du circuit

équivalent qui montre la propagation du bruit, est indiqué dans les figures CF.3(a) et CF.3(b).

Erreur ! Liaison incorrecte.

Figure CF. 3 Circuit équivalent du bruit harmonique: (a)Circuit équivalent avec un filtre passif, (b) Circuit équivalent avec le filtre hybride actif/passif

La performance du filtre actif est évaluée par son rapport d'atténuation, défini par l'équation (C.1)

$$NA = \frac{I'_{in}}{I_{in}} \tag{C.1}$$

I_{in} et I'_{in} sont les bruits du courant qui circule dans le circuit du convertisseur, en présence d'un filtre passif et en présence d'un filtre hybride respectivement. Dans le domaine de fréquence, la fonction de transfert est établie comme suit:

$$I'_{in} = I_n \cdot \frac{R_s \cdot \frac{1}{E} \cdot \frac{1}{sC_{in}} + \frac{1}{sC_s} \cdot \frac{D}{sC_{in}E}}{Z_{in} + R_s\left(1 - \frac{R_s(1+A_vN)}{E}\right) + \frac{1}{sC_s}(1+F \cdot D)} \tag{C.2}$$

$$D = \frac{1}{sL_{in} + \frac{1}{sC_s}} \tag{C.3}$$

$$E = R_s(1+A_vN) + \frac{1}{sC_{in}} \tag{C.4}$$

$$F = -\frac{1}{sC_s} - A_vNR_s\left(\frac{R_s(1+A_vN)}{E} - 1\right) \tag{C.5}$$

La figure CF.4 montre la représentation graphique de la fonction de transfert.

Nous pouvons observer, sur la bande de fréquence concernée (150KHz – 30MHz), que le filtre hybride proposé atteint une atténuation importante de 30dB près de la fréquence fondamentale de commutation du convertisseur, et environ 20dB aux autres fréquences harmoniques. On peut aussi remarquer que l'atténuation du bruit dépend non seulement du caractéristique interne de l'opamp, mais aussi de l'inductance L_{in} placé en parallèle avec le transformateur d'injection. Sur la figure CF.4, on constate que la diminution de la valeur de l'inductance aboutie a une atténuation plus significative du bruit. Cependant, la valeur de l'inductance est limitée par la fréquence de coupure du filtre passif. La fréquence de coupure doit être calculée de telle façon qu'elle soit inférieure à la fréquence de résonance du filtre de sortie du convertisseur pour éviter toute interaction entre les deux filtres qui peuvent aboutir à une oscillation.

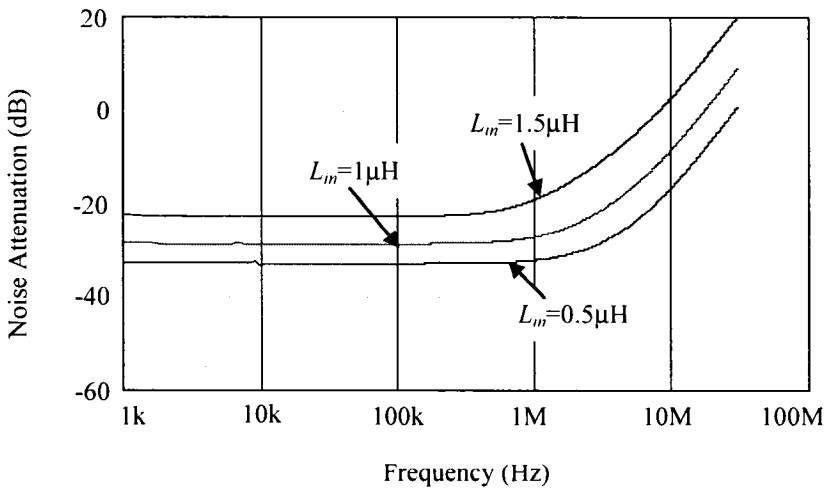

Figure CF.4 Évaluation graphique de l'atténuation du bruit du circuit proposé (Zin=50Ω//50□H, Rs=50Ω, Cs=5□F, Cin=20□F, k1=6·106, k2=100, N=15)

3 Conception du filtre hybride proposé

Les principaux modules qui constituent le filtre hybride proposé sont l'élément de détection, un opamp et un transformateur d'injection. La conception et la sélection de chaque élément sont adressées dans les sous-sections suivantes. Aussi un exemple de conception est donné à la fin de cette section.

3.1 Élément de détection

Pour éviter l'interaction entre le circuit détecteur RC et le filtre passif, il est important que la fréquence de coupure du filtre passe-haut du circuit RC soit inférieure à la fréquence de commutation du convertisseur. La conception du circuit RC suit les procédures conventionnelles de la conception d'un filtre passe-haut. Dans ce cas, la fréquence de coupure du circuit RC est placée à un facteur de 100 inférieurs de la fréquence de commutation du convertisseur.

3.2 Circuit de l'opamp

Le circuit de l'opamp est un élément de contrôle du filtre actif. En effet, l'action du filtre actif doit réduire le bruit incident à zéro, mais en pratique la performance de l'opamp est limitée par sa bande passante (largeur de bande). L'opamp doit opérer avec un gain unitaire pour maintenir sa largeur de bande. Le gain désiré du filtre actif est fourni par le transformateur d'injection. Cependant, à cause des éléments parasites inhérent dans l'opamp, il y'a une erreur de phase et une distorsion du signal à la sortie de l'opamp, en particulier sur la bande à haute fréquence. C'est pour cette raison qu'on ne peut pas avoir une annulation totale du bruit incident. La figure CF.5 montre un exemple d'erreur de

phase introduite par l'opamp lorsque ceci est soumit à un signal d'entrée à haute fréquence. On peut voir que l'erreur de phase est négligeable à 700KHz et elle devient plus significative quand la fréquence augmente.

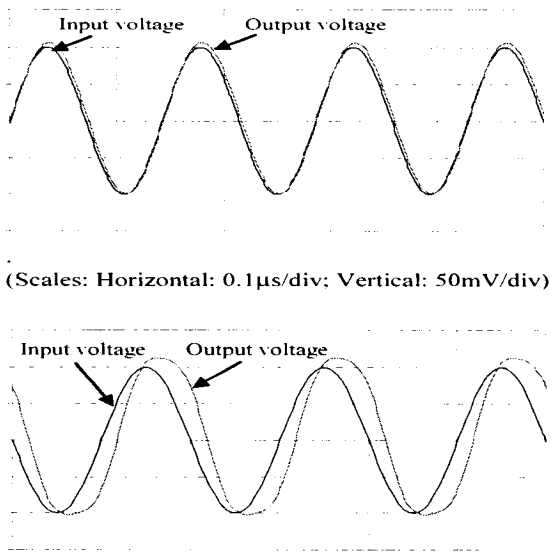

Figure CF.5 Erreur de phase introduite par le circuit opamp: (a) Erreur de phase à une fréquence de 700 KHz, (b) Erreur de phase à une fréquence de 1MHz

Il est important de mentionner que la largeur de bande de l'opamp ne couvre pas nécessairement tout le spectre de la CEM qui est de 150KHz à 30MHz, puisque le bruit diminue de 40dB/décade en haute fréquence. Dans ce cas, il suffit de sélectionner un opamp qui a une bande de fréquence suffisamment haute pour couvrir la fréquence du bruit de l'harmonique fondamentale et les premières harmoniques qui sont multiples de la fréquence fondamentale du convertisseur. Le reste du bruit harmonique, qui se trouve en haute fréquence, sera atténué par le filtre passif.

3.3 Transformateur d'injection

Un transformateur à haute fréquence est utilisé pour injecter le signal du bruit dans la borne positive du convertisseur. Ce signal de bruit de tension est converti en forme de bruit de courant à l'aide de l'inductance du filtre passif qui est connecté aux bornes de l'enroulement secondaire du transformateur. L'inductance du filtre passif avec le transformateur devrait produire une impédance suffisante pour éviter de charger l'opamp. Il est important que le signal injecté soit reproduit par le circuit actif avec une haute précision possible. Sur la figure CF.2, le rapport de transformation est donné comme suit :

$$N = \frac{v_{it\_1}}{v_{it\_2}} = \frac{v_{op}}{v_{it\_2}} \tag{C.6}$$

$$v_{op} = R_s i_{rn} \tag{C.7}$$

$$i_{inj} = \frac{v_{it\_2}}{n\omega_s L_{in}} \tag{C.8}$$

Où n est le nombre de rang du bruit harmonique situé à une fréquence multiple de la fréquence fondamental de commutation du convertisseur qui est de rang n=1. Idéalement

$$i_{inj} + i_{rn} = 0 \tag{C.9}$$

On peut constater que chaque harmonique exige un rapport de transformation différent pour son annulation. Cependant, si on choisit ce rapport de transformation par rapport à la fréquence harmonique fondamentale on peut atténuer aussi les autres harmoniques puisqu'elles sont des multiples de la fréquence fondamentale.

Si on choisit n=1, le rapport de transformation devient :

$$N = \frac{R_s}{\omega_s L_m} \tag{C.10}$$

3.4 Exemple de conception

Un convertisseur de 30W, qui fonctionne avec une fréquence de découpure de 700KHz et une tension d'entrée et de sortie de 28Vdc et 5Vdc respectivement. Un filtre hybride actif et passif est placé à l'entrée du convertisseur. Les valeurs des paramètres du filtre hybride ont été sélectionnées suivant les sections 3.1, 3.2 et 3.3. On retrouve :

$$C_{in} = \frac{1}{(2\pi f_{c\_passive})^2 L_m} = 20\mu F \tag{C.11}$$

$$C_s = \frac{1}{f_{c\_s} R_s} = 5\mu F \tag{C.12}$$

Où R_s=50Ω

Un amplificateur opérationnel (opamp) AD8004 est sélectionné comme élément actif du filtre, à cause de sa largeur de bande, 250MHz avec un gain d'unité. Sa vitesse de balayage est de 3000V/us. De plus, un transformateur d'injection avec un rapport de tours égale à N=15 a été utilisé dans l'expérience.

4 Résultats expérimentaux

Le prototype a été réalisé avec les valeurs des paramètres choisis dans la section précédente. Le prototype opère avec un courant établi à 1 ampère et une sortie constante

de 5Vdc. La figure CF.6 montre le schéma du circuit du prototype qui inclut le filtre hybride.

Erreur ! Liaison incorrecte.

Figure CF.6 Diagramme du circuit proposé

Les tests ont étaient conduits selon les normes de la CEM par rapport aux émissions du bruit conductibles. Les documents des normes consultés sont le EN55011 et le EN55022. La figure CF.7 montre le schéma de montage du test d'émissions conductibles suivant les normes de la CEM.

Erreur ! Liaison incorrecte.

Figure CF.7 Schéma du montage de test d'émission du bruit conductible

Des premiers essais ont été conduits sans le filtre actif. Cependant, le filtre passif est resté connecté aux bornes du convertisseur. La figure CF.8 montre le résultat de cette mesure.

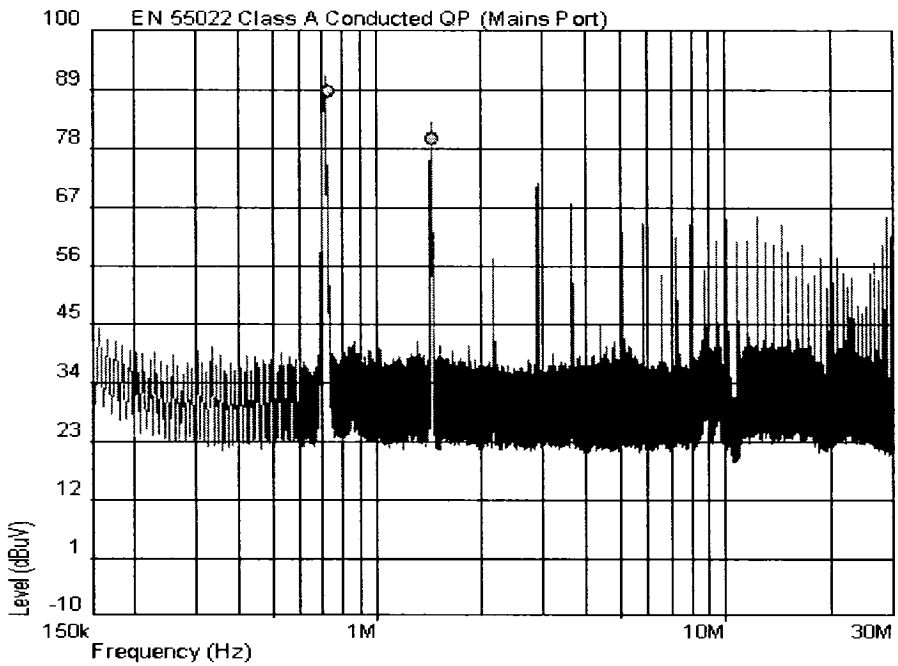

Figure CF.8 Résultat expérimental du bruit conductible aux bornes du convertisseur avec un filtre passif

Afin de confirmer la contribution du filtre actif en matière d'atténuation, un deuxième essai a été réalisé avec la configuration hybride. La figure CF.9 montres le résultat de cet essai. On remarque une atténuation importante de 30dBuV près de la fréquence fondamentale du convertisseur et une réduction du bruit de 20dBuV près des autres fréquences harmoniques. Ces taux de réduction de bruit font une différence significative dans la conformité d'un produit électronique avec les normes de la CEM.

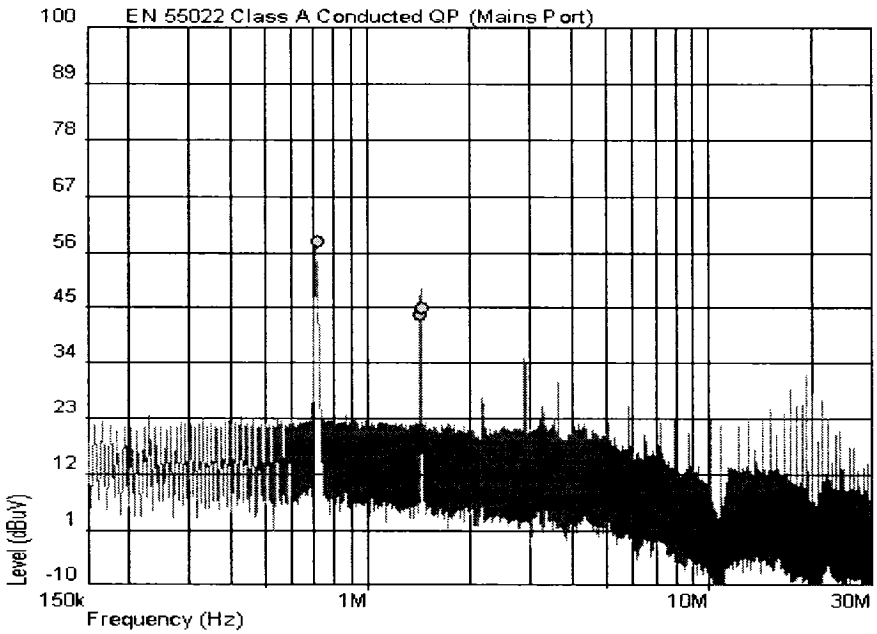

Figure CF.9 Résultat expérimental du bruit conductible aux bornes du convertisseur avec le filtre hybride proposé

Il est à noter que le filtre actif est moins performant dans la région de hautes fréquences à cause de l'introduction de l'erreur de phase et la dépendance du gain du transformateur d'injection. Cependant, le filtre passif a une bonne performance dans cette région de haute fréquence, à cause de sa fréquence de coupure. Le filtre passif est un complément du filtre actif et vise versa.

5 Conclusion

La combinaison d'un filtre d'entrée EMI actif avec un filtre passif traditionnel dans un convertisseur DC/DC a abouti à une réduction importante du bruit d'interférence électromagnétique. Le filtre actif a un impact important dans la réduction du niveau de

bruit près de la fréquence harmonique fondamentale et ses premiers multiples. Cependant, ce type de filtre est moins performant sur la région haute fréquence (>1MHz). Par contre, le filtre passif est plus performant dans la région de hautes fréquences et il est moins performant dans la région de basses fréquences d'où la nécessité d'un filtre hybride passif et actif. Dans une application, tel que l'alimentation en DC dans un satellite, les limites des normes de la CEM permises en matière de bruit conductible sont très strictes, par conséquent un filtre hybride peut fournir une solution viable.

TABLE OF CONTENTS

LIST OF TABLES

LIST OF FIGURES

LIST OF APPENDIX

LIST OF ABREVIATONS AND SYMBOLES

ABREVIATIONS

EMI	Electro-Magnetic Interference
EMC	Electro-Magnetic Compatibility
EMD	Electro-Magnetic Disturbance
DC/DC	Direct Current to Direct Current Conversion
FCC	Federal Communications Commission
DOD	Department Of Defense
EEC	European Economic Community
CISPR	Comité Internationale Spéciale Pour Radio
IEC	International Electro technical Commission
ZVS	Zero Voltage Switching
PFC	Power Factor Correction
PWM	Pulse Width Modulation
PCB	Printed Circuit Board
IL	Insertion Loss
CM	Common Mode
DM	Differential Mode
MOSFET	Metal Oxide Semiconductor Field Effect Transistor
LISN	Line Impedance Stabilization Network
CCCS	Current Controlled Current Source
FFT	Fast Fourier Transform

SYMBOLES

U_0	The generator noise voltage
U_m	The measuring instrument noise voltage
U_1	the measured noise voltage without the EMI filter

U_2	the measured noise voltage with the EMI filter
R_1	The generator source impedance
R_2	The measuring instrument input impedance
ω_o	The self-resonant frequency of the LC input filter
ω	The angular resonant frequency
C_d	Damping capacitor
R_d	Damping resistor
Z_{DC}	The output impedance of the input DC source
Z_{IF}	The filter input impedance with the output port open
Z_{OF}	The filter output impedance with the input port shorted
Z_{in}	The input impedance of the DC/DC converter
I_n	The ripple current generated by the switching elements
I_{in}	The injected noise current
L_{in}	Input filter inductor
C_{in}	Capacitor of the input passive filter
R_s	Sense resistor
C_s	Sense capacitor
A_v	The closed-loop voltage gain
A_i	The closed-loop current gain
A(s)	Frequency-dependant open-loop gain function
k_1	The DC open-loop voltage gain
k_2	The cutoff frequency open-loop voltage gain
v_{it_1}	Injection transformer primary windings voltage
v_{it_2}	Injection transformer secondary windings voltage
v_{op}	The opamp output voltage
ω_s	The DC/DC converter switching frequency
i_{rn}	The input ripple current
i_{inj}	The injected current noise
N	Transformer turns ratio

f_{c_s}	Cut-off frequency of the sense circuit

Chapter 1

Introduction

To further clarify the content of this thesis project, it is important to define the basic concepts surrounding this subject. These are namely Electromagnetic Interference (EMI), which is the problem and Electromagnetic Compatibility (EMC) which is the requirement that needs to be met. EMI is regarded as the unacceptable high-level Electromagnetic Disturbance (EMD) that can prevent electrical and electronic devices, apparatus, and systems from operating as intended in an electromagnetic environment. In the contrary, EMC is the ability of an electronic or electrical device to operate or to function as prescribed reliably in the presence of electromagnetic environment, and at the same time, the device should confine its internally generated EMI to avoid interference with other devices in the vicinity.

1.1 EMI generation in DC/DC converter

A DC/DC converter is a switch-mode power converter with rapid changes in voltages and currents. These switching waveforms contain significant energy levels at the switching and harmonic frequencies and therefore generate EMI problems. The EMI is transmitted in two forms: radiated and conducted. Usually the conducted noise is several orders of magnitude higher than the radiated noise into free space. The conducted noise consists of two categories commonly known as the differential mode and the common mode. The

differential-mode noise is a current or a voltage noise measured between the lines of the source. The common-mode noise is a current or a voltage noise measured between the power lines and the ground. Both the differential-mode and common-mode noises are taken into account in the EMI filter design.

1.2 EMI standards

Various regulations have been imposed by government authorities to limit the level of the EMI emissions. These regulations have been developed as EMC standards and are a condition to product marketing and circulation. A product is considered to be conformant when the limits applying to that product are not exceeded. A distinction should be made between products manufactured on a one-time basis and a mass production. For the one-time products, each single unit must comply 100% with the limits values. Whereas, the series products are required to have a margin of 2dB below the limit value, in order to be considered compliant.

In North America, the authority that sets these limits is the Federal Communications Commission (FCC) and the Department Of Defense (DOD). In Europe, all standards are set by the European Economic Consortium (EEC). There is also an international body called the Comité International Spécial Pour Radio (CISPR), and the International Electro-technical Commission (IEC), which has no regulatory authority but it can set standards that can then be adopted by individual nations in order to facilitate international trade.

1.3 EMI reduction

The most cost-effective way of reducing EMI is to prevent it from being generated at its source. For examples, the noise generation can be reduced by selecting a proper topology of DC/DC converters, soft-switching, zero-voltage switching (ZVS), using Power Factor Correction (PFC) controller when it is possible and utilizing Pulse-Width Modulation (PWM) controller that uses Spread Spectrum techniques to minimize the rate of the di/dt or the dv/dt. If these preventive techniques did not remedy the problem, a proper attenuation and/or cancellation method can be employed.

To reduce the conducted noise to an acceptable level, an EMI filter circuit can be introduced at the input leads of the converter. Standard EMI filters are passive LC low-pass circuits with serial inductor (high impedance) and parallel capacitor (low impedance). Within the EMI filter category, to meet special requirements, a multistage EMI filter may be implemented.

The major criteria in designing passive EMI filters, is determining the most economical circuit configuration that gives a high insertion loss in the frequency range of 0.15 to 30 MHz and is capable of withstanding the DC current and voltage ratings. However, there are three major constraints in meeting those criteria. First, the total capacitance value is limited, for safety reason, only small amount of leakage current is allowed that can flow through the safety ground. Secondly, the series inductance can results in power loss, due

to its DC copper resistance and the circulating current in the magnetic core. Finally, the inductor must be designed as bulky as possible to ovoid saturation.

1.4 Industrial trends

The mutual relationship between the industry and the academic research has played a major role in the evolution of the commercial products. This section provides a brief overview on the commercially available EMI filters and their manufacturers to better understand the area in which this research has been contributed.

Among the top EMI filters manufacturers, Picor Corporation is perhaps the first company that introduced the active filter in DC/DC converters in one single package (Picor, 2006). However, it is not known what type of internal configuration the active filter has. From the data sheet, the active filter exhibits a good performance in terms of insertion loss at 250 KHz (>60 dB) and with their small footprints, a great deal of board real estate can be recuperated. The QPI active filters series are intended to be used with passive Y-capacitors and require a series resistor between the filter shield and the converter shield. The absence of these connection requirements will degrade dramatically the performance of the active filter.

Another well known manufacturer in the field of EMC is SCHAFFNER (SCHAFFNER, 2006). The company has been around for decades, producing state of the art EMI line filters for most types of power distribution. The FN EMI filter family is the passive filter with single, two or more stages of LC low-pass circuits. They are manufactured in

different packaging types: open frame, PCB mount, and standalone with significant insertion loss up to 70dB at higher frequencies. These passive filters can not be used where the PCB real estate is the prime design requirements in DC/DC converters.

Texas Spectrum Electronics specializes in high quality custom filters to meet specific military and aerospace requirements (Texas Spectrum Electronics, 2006). It also provides the same quality, cost effective filter products to commercial and industrial customers. The CF filters family, is based on passive LC low-pass circuits that can be connected at the input of the DC/DC converters. From the data sheet, these filters have a current rating ranging from 1 to 20 Amps and a maximum common mode insertion loss of 55 dB around 10 MHz. However, the size of these passive filters can be equal to the size of a low profile (small footprints) DC/DC converter.

1.5 Master Thesis objectives and outlines

The scope of this master thesis deals with the subject of satisfying the EMC requirements in terms of conducted noise emissions at the input leads of a DC/DC converter. The research work is focused on the design and implementation of a hybrid EMI filter as a novel solution for conducted EMI mitigation by adding an active circuitry to the existing passive circuit to reduce its size and cost as well as to improve the overall performance of the input EMI filter. The design prototype is installed into a DC/DC converter to evaluate its performance in terms of conducted noise attenuation. The design of the DC/DC converter has been realized to serve as a platform for the hybrid filter testing and it is not the main focus of this work.

This master thesis starts by stating the reason for selecting the input hybrid (combined active and passive) filter over a single passive or active output filter. EMI generation and EMI passive filters have been described. Brief discussions about the commercially available EMI filters are presented. Different techniques of conducted EMI mitigation, using active and passive circuits, have been explored. Chapter 3 provides a detailed analysis and design of the proposed combination of active and passive filter, as well as experimental results. Chapter 3 has been submitted as a journal publication to the IEEE Transactions on Industrial Electronics. Measurement tests are included in Chapter 4 to demonstrate the validity of the experimental results. Finally, in Chapter 5, a conclusion is drawn to present an evaluation on the performance of the proposed hybrid filter. Recommendations for future research are also part of this chapter.

Chapter 2

Overview of passive and active filters

2.1 Introduction

There are many ways of EMI noise mitigation, depending on the location of the interference source, the EMI noise can be reduced by proper selection of the circuit topology, proper circuit grounding and by filtering. This later is the most commonly used method for EMI noise reduction when the DC/DC converters fail to achieve the electromagnetic compliance requirements in terms of conducted noise emissions. Passive EMI filters were first introduced in 1950s to respond to the EMC legislation set forth by the ITC to suppress EMI caused by electronic equipment. This legislation was reflected into EMC standards which limit the level of EMI emissions from the electronic equipment. Since then passive EMI filters have been evolved into different sizes and shapes to comply with the continuously changing and challenging limits of the EMC standards.

The idea of an EMI filter is to block, or bypass the interference noise, which can be achieved by introducing high impedance (inductor) into the path of the interfering currents and bypassing them to ground through a low impedance (capacitor) path. This technique is called passive filtering, since it uses only passive components in the circuit. This type of filters is simple and cost effective in some applications; however, in

application where stringent noise reduction is required, the size, weight, temperature and reliability can present a significant design challenge.

An alternative solution to the conventional approach is the use of an active EMI filter which uses active components such as opamp to reduce the EMI noise. This technique samples the noise signal, and then inverts it and injects it back into the circuit. The EMI noise is reduced by superposition of two signals with the same magnitude and opposite phase. However, the performance of this technique is limited by the frequency characteristics of the active components at higher frequencies.

In this chapter, the conventional passive filters are introduced in section 2.2. In this section, the circuit configuration and design considerations in terms of mismatch impedances, components selection and stability are presented. Section 2.3 describes the circuit operation, performance and the limitations of the output active EMI filter. Finally, in section 2.5, discuss some advantages of choosing the input hybrid (active and passive) EMI filter over the existing output active EMI filter.

2.2 Passive EMI filters

In order to comply with the International EMC standards, DC/DC converter circuits using high-frequency switching devices, such as MOSFET, must carry a proper EMI filter to avoid the injection of excessive conducted noise towards the power network, in the frequency range of 150 KHz – 30 MHz. The desired noise attenuation is achieved by

means of suitable passive EMI filter connected in the supply section between the DC bus and the DC/DC converter.

A passive EMI filter is essentially an inductor-capacitor (LC) network designed to attenuate high frequency interference while at the same time allow the low frequency operating current to pass through unaffected. The filtering action comes from the impedance characteristics of the inductor and capacitor. The impedance of an inductor increases with frequency; while the impedance of a capacitor decreases as frequency increases. This can be deduced from equations 2.1 and 2.2 respectively.

$$X_L = 2\pi fL \tag{2.1}$$

$$X_C = \frac{1}{2\pi fC} \tag{2.2}$$

It is important to note that the basic approach to EMI filtering is to use a set of series inductors and parallel capacitors to divert the flow of EMI currents away from the victim circuit. This is done by using the high inductor impedance to prevent the flow of the EMI noise from flowing in the circuit and the low capacitor impedance to divert the EMI noise towards the ground. The EMI current flows through the path of the least impedance.

Hence, filtering common-mode EMI requires capacitors connected to earth. These capacitors are referred as Y capacitors and safety regulations limit these capacitors to relatively low values. Consequently, high values of inductance are essential for effective filtering. However, differential-mode filtering requires capacitors across the input lines.

These capacitors are referred as X capacitors. The detailed circuit configurations and design considerations are described in the following sections.

2.2.1 Basic Circuit Configurations

The basic passive EMI filter circuit configurations are shown in Figure 2.1. The π-circuit configuration is the most common one. However, in high performance applications, multistage circuit configurations are also used. Configurations with more than three stages are not recommended due to their excessive space and power losses.

To suppress the EMI noise in both positive and negative lead, one of the selected filter circuits of Figure 2.1 must be inserted in each input lead of the DC/DC converter. Therefore, the two-port network EMI filter becomes three-port network with the ground lead added to the filter circuit, as shown in Figure 2.2. In this configuration, both common-mode (CM) and differential-mode (DM) noises can be attenuated.

Erreur ! Liaison incorrecte.

Figure 2.1 Basic passive EMI filter circuit configurations: (a) single stage LC-circuit, (b) π-circuit, (c) T-circuit, (d) Multistage LC-circuit

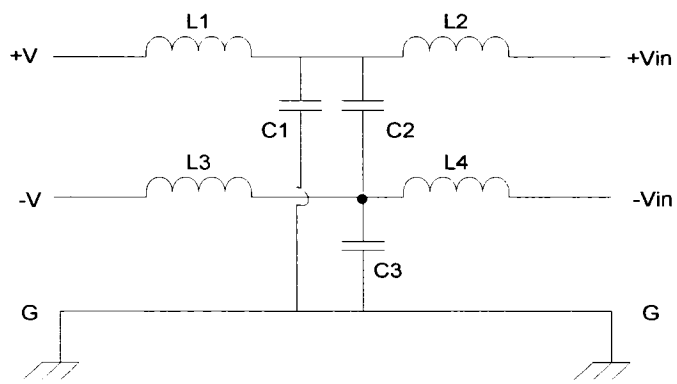

Figure 2.2 Basic EMI filter Configuration for CM and DM attenuation

The passive EMI filter can be evaluated by its insertion loss which can be defined as the ratio of the generator voltage and the measured voltage when the filter is inserted between the generator and the measuring instrument as shown in Figure 2.3.

The insertion loss (IL) can be generally expressed in terms of voltages as:

$$IL = 20\log\left[\frac{U_1}{U_2}\right] \tag{2.3}$$

where: U_1 and U_2 are the noise voltages without the filter and with the filter respectively.

According to figure 2.3, with R_1 the generator source impedance, and R_2 the measuring instrument input impedance, the insertion loss expression becomes:

$$IL = 20\log\left[\frac{U_0}{U_m}\times\frac{R_2}{R_1+R_2}\right] \tag{2.4}$$

Where U_0 is the generator voltage and U_m is the measuring instrument voltage when the filter under test is inserted in the circuit.

In practice, R_1 and R_2 should be equal; in this case equation (2.4) can be simplified as follows:

$$IL = 20\log\left(\frac{U_0}{2\times U_m}\right) \tag{2.5}$$

The attenuation is a transfer function that reflects the performance of the filter at each frequency with the real circuit impedance, rather than assumed impedance as in the case of the insertion loss measurements. To respond to the challenges of the low profiles DC/DC converters and their fast growing switching frequency (>1MHz), it is important to consider the following parameters: the size (small footprint), performance (at least 30

dB attenuation across the frequency spectrum) and cost. The first two parameters are circuit related and provide a lot of room for research on the combination of the passive and the active EMI filters as an integral part in an open frame configuration of DC/DC type converter.

Erreur ! Liaison incorrecte.

Figure 2.3 Insertion loss (IL) measurement: (a) Reference circuit, (b) Filter under test inserted

2.2.2 Mismatch impedances

One of the main problems in designing passive EMI filters for DC/DC converters is caused by the arbitrary selection of the source and the load impedance values. This means that there is no guarantee that the arbitrary selected values that suppose to reflect the source and the load impedances are valid values, given that a typical EMI filter is to be installed in DC/DC converters which can be used in variety of applications and supply networks. The high frequency impedance of the DC/DC converter which represents the noise source varies widely, depending on the converter circuit topology, circuit layout, types of MOSFET and the switching frequency. Furthermore, the load impedance which is the supply impedance of the passive EMI filter is even less predictable than the source impedance. Because the load impedance depends on the facility network from which the DC/DC converter would be supplied and varies with the number of electrical equipment connected to the supply network.

To clarify the mismatch impedance issue, it is important to illustrate the insertion loss of a single stage LC-circuit at various load impedances. For simplicity, the source impedance is assumed to be very small.

2.2.3 Resistive load impedance

Figure 2.4 shows the circuit diagram with the LC filter connected to resistive load impedance.

Erreur ! Liaison incorrecte.

Figure 2.4 LC filter connected to a resistive load

In the frequency domain, the insertion loss $IL_R(\omega)$ of the EMI passive filter can be derived using equation (2.3).

$$IL_R(\omega) = 20\log\sqrt{\left(1-\frac{\omega^2}{\omega_0^{\,2}}\right)^2 + \frac{(\omega L_1)^2}{R_1^{\,2}}} \tag{2.6}$$

where ω_o is the self-resonant frequency of the LC circuit, ω is the angular resonant frequency of the circuit, L_1 is the inductance of the passive filter, and R_l is the load resistance.

To demonstrate the effect of the resistive impedance on the performance of the EMI filter, the equation above is plotted for different values of the resistive load impedance. This is shown in Figure 2.4. It can be seen that the insertion loss does not change dramatically above the desired frequency of interest (10 KHz) which corresponds to a minimum insertion loss (IL_{min}). However, a large dip below zero magnitude (negative

side) appears due to the resonance of the LC circuit. As a result, the EMI noise in this region will be amplified instead of suppressed.

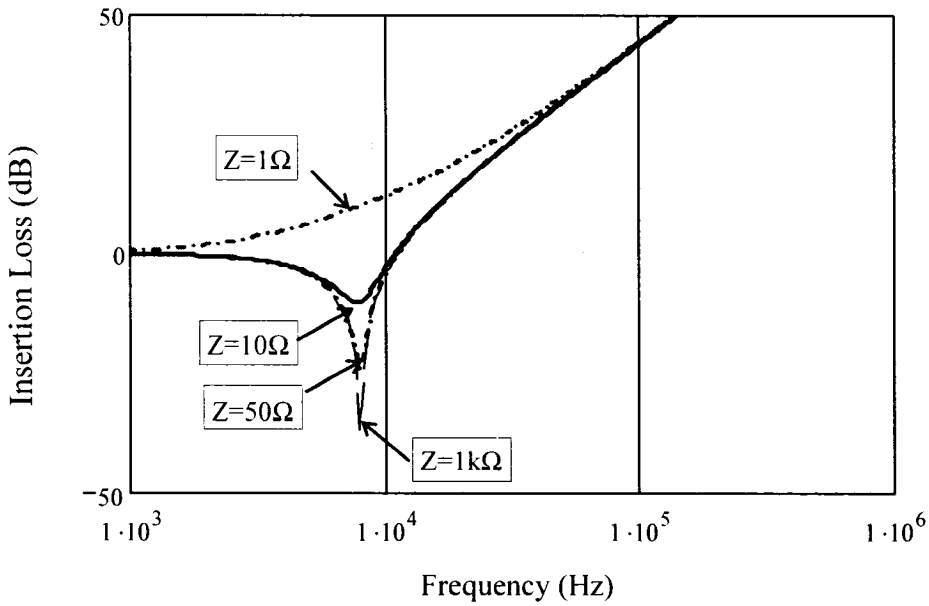

Figure 2.5 Insertion loss vs. frequency for different values of resistive load impedances (L_1 = 10μH, C_1 = 1 μF, Z = R_1)

2.2.4 Inductive load impedance

Figure 2.6 shows the LC filter connected to the resistor in parallel with an inductor.

Erreur ! Liaison incorrecte.

Figure 2.6 LC filter connected to inductive impedance

The resonant frequency of the inductor load in terms of ω_o is given by:

$$\omega_L^{\ 2} = \omega_o^{\ 2}\left(1+\frac{L_1}{L_L}\right) \tag{2.7}$$

where L_1 is the inductance of the LC circuit and L_L is the load inductance.

The insertion loss of the circuit shown in Figure 2.5 is given by:

$$IL_{RL}(\omega) = 20\log\left[\left(\frac{\omega_L}{\omega_0}\right)^2\sqrt{\left(1-\frac{\omega^2}{\omega_L^2}\right)^2+\frac{(\omega L_1)^2}{R_1^2}\times\frac{\omega_0^2}{\omega_L^2}}\right] \tag{2.8}$$

Figure 2.6 illustrates the effect of the inductive load impedance on the insertion loss of the LC passive filter. Comparing with Figure 2.4, it can be seen that the resonant frequency of the circuit has increased beyond the desired frequency of interest (10 KHz) and the amplification of the EMI noise can occur in this region. This is the worst case scenario in which the EMI filter could be installed.

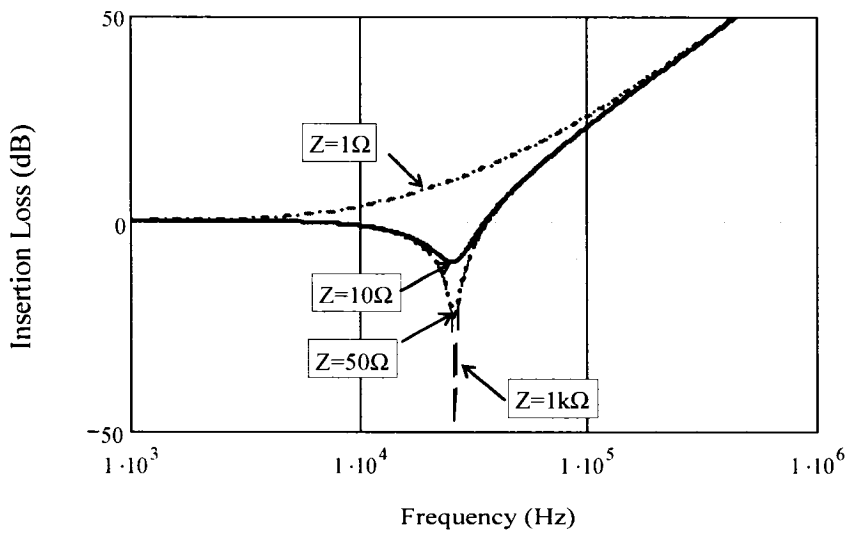

Figure 2.7 Insertion loss vs. frequency for different inductive load impedances

(L_1 = 10μH, C_1 = 1μF, L_L = 1μH, Z = R_1//L_L)

2.2.5 Capacitive Load impedance

The third case of mismatched impedance is the capacitive load impedance, in which the LC filter is connected to a resistor in parallel with a capacitor. The circuit diagram is shown in Figure 2.8.

Erreur ! Liaison incorrecte.

Figure 2.8 LC filter connected to capacitive impedance

The resonant frequency of the capacitive load in terms of ω_0 is given by:

$$\omega_c^2 = \frac{\omega_0^2}{1+\frac{C_L}{C_1}} \tag{2.9}$$

where: C_L is the load capacitance.

The LC circuit insertion loss in this case can be described by:

$$IL_{RC}(\omega) = \sqrt{\left(1-\frac{\omega^2}{\omega_c^2}\right)+\frac{(\omega L_1)^2}{R_1^2}} \tag{2.10}$$

Figure 2.9 shows the insertion loss of the EMI filter as a function of frequency for different values of the load impedance. As a result of the load being capacitive in nature, the resonant frequency is decreased compared with the resistive load of Figure 2.5. Thus the insertion loss at the desired frequency (10 KHz) has increased.

The load impedance variations mentioned above are important criteria to be accounted for when installing a passive EMI filter in a given power supply. This is to say that the

actual insertion loss of a passive EMI filter, because of the mismatch impedances, can differ from the calculated results of matched conditions.

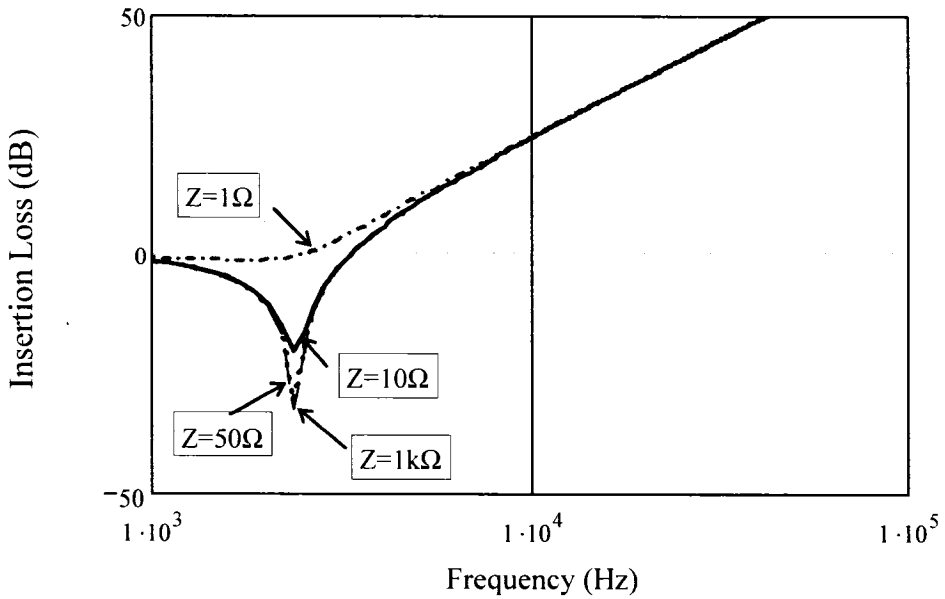

Figure 2.9 Insertion loss vs. frequency for different capacitive load impedances

(L_1 = 10μH, C_1 = 1μF, C_L = 10μF, Z = R_1//C_L)

2.2.6 Components selection

In this section, the basic procedures of designing and selecting the components of the passive EMI filter are presented. To show the performance of the passive EMI filter, in terms of attenuation, an example will be taken to further quantify the filter circuit performance.

Figure 2.10 shows the equivalent circuit of the passive EMI filter; the purpose of the damping resistor R_d is to reduce the output impedance of the filter at the cut-off frequency. The damping capacitor C_d across the DC bus prevents the problem of voltage overshoots and ringing at the input of DC/DC converter. The input of the DC/DC converter is represented by impedance R_{in}. The impedance of a passive EMI filter is defined as follows:

Erreur ! Liaison incorrecte.

Figure 2.10 Single stage passive EMI Filter diagram

$$Z_1 = R_f + sL_f \tag{2.11}$$

where R_f and C_f are series resistance and filter inductance respectively

$$Z_2 = ESR_{C_f} + \frac{1}{sC_f} \tag{2.12}$$

where ESRc is the equivalent internal series resistance of the filter capacitor

$$Z_3 = \frac{1}{sC_d} + ESR_{C_d} + R_d \tag{2.13}$$

Then the equivalent impedance of the EMI filter at the input of DC/DC converter is given by:

$$Z_{eq} = Z_1 + \frac{Z_3 Z_2 R_{in}}{R_{in} Z_3 + R_{in} Z_2 + Z_2 Z_3} \tag{2.14}$$

The values of damping resistor and energy-storage capacitor can be selected according to:

$$R_d \approx \sqrt{\frac{L_f}{C_f}} \tag{2.15}$$

$$C_d \approx 2 \cdot C_f \tag{2.16}$$

Figure 2.11 shows the main circuit waveforms of a DC/DC converter. The current waveform at the secondary of the transformer is a square-wave due to the switching device M1, (see schematic diagram in Appendix B). This square-wave is characterized by its peak current I_P, duty cycle D, its switching frequency F_s, and its rise/fall time.

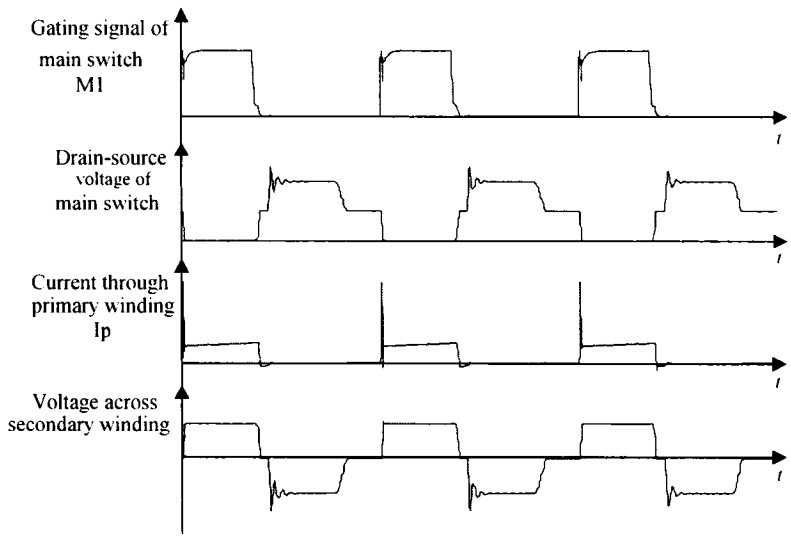

Figure 2.11 Main operating circuit waveforms

To evaluate and attenuate the level of the conducted EMI disturbances, it is important to know the Fourier coefficients of the current square-wave. Taking the Fourier transform of the current signal, we obtain the fundamental harmonic current, or the first harmonic content.

$$I_{fund} = 2I_p D \frac{\sin(\pi D)}{\pi D} \frac{\sin(\pi t_r / T)}{\pi t_r / T} \tag{2.17}$$

where, I_p is the peak current; D is the pulse duty-cycle; T is the pulse period, and t_r is the pulse rise time.

Suppose that the DC/DC converter is required to be compliant with the EN55022 class-A conducted emission standards (EN55022, February 1995), as shown in Figure 2.12. These standards require that noise level must be below the limit line of 66 dBμV in the frequency range of 150-500 kHz and 60 dBμV in the frequency range of 500 kHz – 30 MHz.

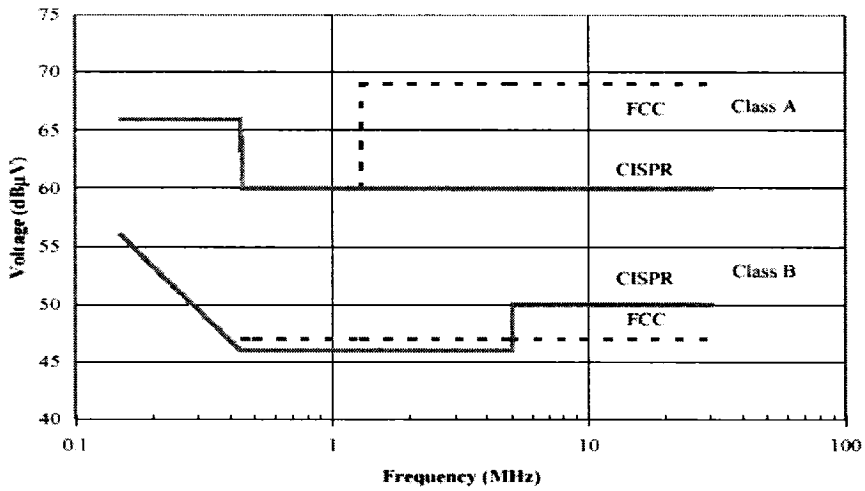

Figure 2.12 Limit lines of conducted emissions class A & B equipment (ANSI C63.022)

As an example, suppose that a DC/DC converter with an input peak current of 2A. This current is characterized by a 25ns rise/fall time and a 50% duty cycle. The switching frequency is 500 KHz. The calculation can be split into the following steps:

1. Evaluate the fundamental current from equation (2.17): I_{fund} = 588 mA

2. Convert the fundamental current into voltage using the capacitor's ESR around 100mΩ:

$$V_n = I_{fund} R_{esr} = 58.8 \quad mV \tag{2.18}$$

In terms of dBμV:

$$V_n = 20\log(0.0588 \times 10^6) = 95 \quad dB\mu V \tag{2.19}$$

3. Select a target noise level and deduce the desired attenuation level:

60 dBμV is the maximum limit imposed by the EN55022 at 150 KHz. If we take a 45 dBμV as a target level, including a safe margin, this will yield to a required attenuation of: 95 – 45 = 50 dBμV to be attenuated.

4. Calculate the corner frequency F_c of the LC low-pass filter that will lead to 50 dBμV attenuation at F_s = 500 KHz according to:

$$-50 = -45\log\left(\frac{F_s}{F_c}\right) \tag{2.20}$$

F_c = 38.8 KHz can be obtained.

5. Select a filter capacitor value to be C_f = 100nF.

6. From $F_c = \frac{1}{2\pi\sqrt{L_f C_f}}$, extract the value of L_f = 168μH.

7. Select an inductor with the calculated value that can withstand the input current of 2 Amps. This can be found in the Manufacturer Data Sheet.

2.2.7 Input impedance consideration

The input and the output impedances of the passive EMI filter are important parameters that must be known when connecting the filter to the input side of the DC/DC converter. This condition sets a boundary requirement between the EMI filter and the DC/DC converter in terms of input/output impedances. As demonstrated by (Middlebrook, 1976), the input EMI filter can adversely amputate the performance of the DC/DC converter which can be driven into continuous oscillations and instability. Thus, the input passive EMI filter should be designed with the issue of the impedance compatibility in mind. Figure 2.13 shows the interface impedance of the input passive EMI filter with the input DC voltage bus and the DC/DC converter.

Erreur ! Liaison incorrecte.

Figure 2.13 Interface impedances of the passive EMI filter

In Figure 2.13, the parameters are defined as:

Z'_{IF}: Input Impedance of the passive EMI filter loaded with the DC/DC converter;

Z'_{OF}: Output Impedance of the passive EMI filter connected to an input DC bus;

To ovoid the issue of interaction of the EMI filter with its load converter, the following input/output impedance compatibility requirements must be satisfied (Choi et al., 1995):

1. At the interface between the DC source and the input filter:

$$|Z_{DC}| \leq |Z'_{IF}| \tag{2.21}$$

Where, Z_{DC} is the output impedance of the input DC source, and Z'_{IF} is the input impedance of the filter with the output port open

2. At the interface between the input filter and the DC/DC converter:

$$|Z'_{OF}| \leq |Z_{in}| \tag{2.22}$$

Where, Z'_{OF} is the output impedance of the filter with the input port shorted, and Z_{in} is the input impedance of the DC/DC converter.

Since impedances Z_{DC} and Z_{in} are system dependant and can not be known, the two impedances Z'_{IF} and Z'_{OF} can be considered as design parameters and can be calculated or measured.

Based on the impedance condition stated above, one can design the EMI filter taking into account the input and the output impedances of the passive filter. The input impedance can be selected as high as possible to minimize interactions with the input DC bus, and the output impedance can be selected as low as possible to minimize interactions with the loop gain of DC/DC converter.

2.2.8 Performance and limitations of the Passive EMI filter

Passive filtering can be considered as the most economical solution in many applications, in particular where space and weight do not constitute a prime obstacle in the design specifications. The availability of the components and the design simplicity permit the manufacturers to include passive filters in almost all DC/DC converters. However, their performance is strongly dependant on the source and the load impedances which are most of the time assumed quantities in the case of the Off-the-Shelf products and they are measured quantities in the case of integrated design. In addition, to prevent resonance of

the LC filter, a damping resistor must be introduced in the circuit. This will reduce the efficiency of the DC/DC converter and result in a permanent current circulation at no-load condition. One of the features that make the passive EMI filter selective is their performance at higher frequencies (> 1MHz). This is due to the series inductive impedance which is directly proportional to the frequency. Furthermore, for safety and shock hazards, the total capacitance is limited to a maximum value so that the capacitor leakage current finds its way to the chassis ground.

These limitations are usually very strict, and it can be very difficult to meet them while achieving the insertion loss objectives. Therefore, in certain application where the size, weight and thermal dissipation are crucial design requirements, the passive filter simply can not be an appropriate contingent.

2.3 Active EMI filters

An active EMI filter is an electronic circuit that cancels the input current ripple/noise generated by switched mode DC/DC converters. The EMI noise suppression is based on the superposition of two waves with equal magnitude and opposite phase. This can be achieved by sensing the noise signal, and then inverting this noise with an op-amp inverter and injecting the replicated noise signal back to the input bus of the DC/DC converter.

2.3.1 Circuit Operation

The active EMI filter circuit is specified by three main feedback loop elements: the sensing element, the control element and the injection element. The current/voltage noise is sensed through an RC branch for sensing the noise voltage or across a sense transformer in case of current sensing. The sensed current/voltage noise is fed into the control element, which merely an op-amp with high bandwidth and low distortion capabilities, to be inverted to produce a 180 degrees phase shift in the range of the frequency of interest (150 KHz – 30MHz as per CISPR22 EMC standard). The inverted current/voltage noise is then injected back into the input bus of the DC/DC converter to cancel the incident current/voltage noise. However, to obtain an optimum noise attenuation/cancellation, it is required that the sensed noise be reproduced with high fidelity without or minimum distortion. Various active EMI circuit configurations in terms of sensing and driving parameters are shown in Figure 2.14. Although these basic circuit configurations achieve the same function by canceling the noise current/voltage from the input of the DC/DC converter, they do have some advantages and drawbacks from a practical point of view. These configurations can be selected depending on the application, the components count and the available space on the PCB.

To compare the effectiveness of the active circuits shown in Fig.2.14, the noise attenuation for each category of the active circuit should be calculated. Hence, the four configurations of the active circuits can be represented by their equivalent circuit according to their driving parameter (current or voltage injection), either voltage or

current driving. Figure 2.15 (a) shows the equivalent circuit of the voltage injected noise which corresponds to Figures 2.14(a) and (c). Whereas Figure 2.15(b) shows the equivalent circuits of the current injected noise which correspond to Figure 2.14(b) and Figure 2.14(d).

Erreur ! Liaison incorrecte.

Figure 2.14 Active EMI circuit configurations: (a) current sensing/Current driving; (b) Current sensing/Voltage driving; (c) Voltage sensing/Current driving, (d) Voltage sensing/Voltage driving

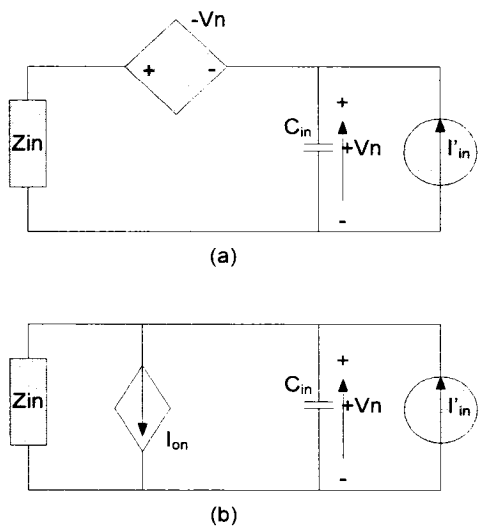

Figure 2.15 Equivalent representation of the active circuit: (a) Voltage noise injection, (b) Current noise injection

The noise attenuation can be defined as:

$$NA = \frac{I'_{in}}{I_{in}} \tag{2.23}$$

where I'_{in} and I_{in} are the input noise current with and without using the active circuit respectively.

In Figure 2.15, when the active filter is not employed in the circuits of Figures 2.15(a) and 2.15(b), the input noise current can be given by:

$$I_{in} = I_n \cdot \frac{1}{1 + sC_{in}Z_{in}} \tag{2.24}$$

Where C_{in} is the sense capacitor and Z_{in} is the source impedance.

In Figure 2.15 (a), when the voltage injected active filter is used, the input noise current is derived as:

$$I'_{in} = I_n \frac{1-K}{1-K+sC_{in} \cdot Z_{in}} \tag{2.25}$$

where K is a function of the open-loop voltage gain of the active device (opamp), A_v.

$$K = 1 - \frac{1}{1 + A_v} \tag{2.26}$$

And,

$$A_v = \frac{k_1}{1 + s/k_2} \tag{2.27}$$

where k_1 is the DC open-loop voltage gain (typically 10^5 to 10^7), and k_2 reflect the cutoff frequency. These two parameters describe the frequency-dependant open loop characteristics of the selected opamp.

Therefore, the noise attenuation of circuit of Figure 2.15 (a) can be calculated as:

$$NA_v = \frac{1-K}{1-K+sC_{in}\cdot Z_{in}}\left(1+sC_{in}\cdot Z_{in}\right) \tag{2.28}$$

Figure 2.16 show the plot of the noise attenuation for the voltage injected active filter with different values of k_1 and k_2.

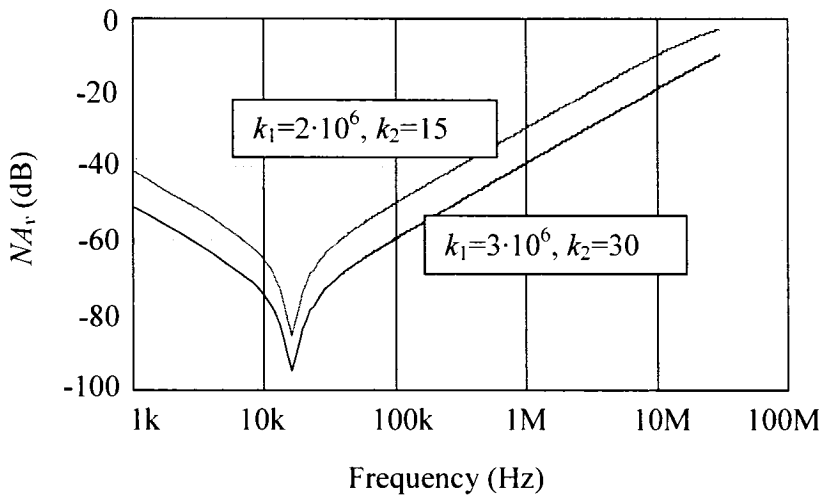

Figure 2.16 Noise attenuation of the voltage injected active filter

(Zin = 100Ω//100μH and C_{in} = 0.1μF)

For an ideal opamp circuit, k_1 and k_2 tends to infinity, and the voltage gain K will tends to unity, hence, the resultant input noise current will reduce to zero. However, in practice, the opamp device circuit due to its parasitic effects at high frequency, the gain-bandwidth product will limit the active filter performance. From Figure 2.16, it can be seen that the opamp with higher DC gain and higher cut-off frequency can result in better noise attenuation.

For circuit (b) of Figure 2.15, when the current injected active filter is used, the input noise current is derived as:

$$I'_{in} = \frac{(1-G)\cdot I_n}{1+sC_{in}\cdot Z_{in}} \tag{2.29}$$

where G is a function of the open-loop current gain of the active device (opamp) used in the circuit, namely A_i, which is identical to A_v defined in equation (2.26)

$$G = 1 - \frac{1}{1+A_i} \tag{2.30}$$

Hence, the noise attenuation of the circuit (b) of figure 2.15 is given by:

$$NA_i = 1 - G \tag{2.31}$$

Figure 2.17 shows the plot of the noise attenuation for the current injected active filter with different values of k_1 and k_2

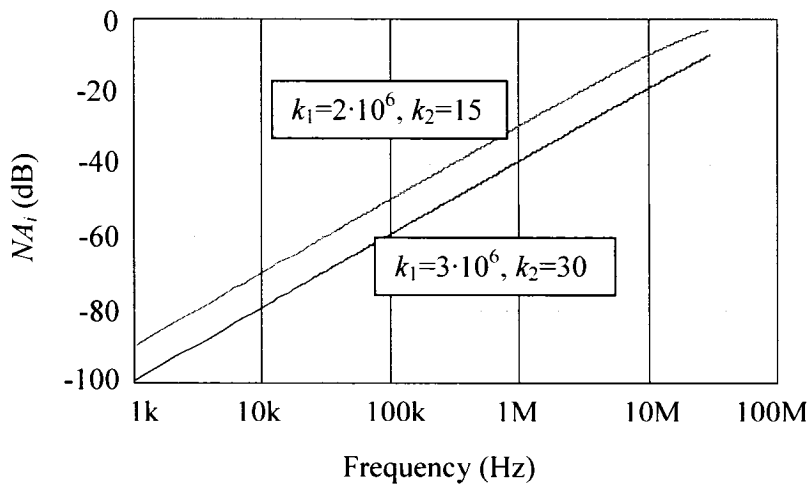

Figure 2.17 Noise attenuation of the current injected active filter

(Zin = 100Ω//100μH and C_{in} = 0.1μF)

Similarly, for an ideal opamp circuit, the current gain G will approach a unity value and the input noise current will reduce to zero. Practically, from Figure 2.17, the opamp with higher DC gain and higher cut-off frequency will result in better noise attenuation.

2.3.2 Performance and Limitations

Active EMI filter has a distinctive performance at low frequency which can be translated as a substantial reduction in EMI noise in the frequency range of 100 KHz to 1MHz. This is mainly due to the unity gain of the opamp which forms the control element of the active filter, at low frequency. Depending on the switching frequency of the DC/DC converter, the active EMI filter can be designed to suppress low frequency harmonic components which can not be attenuated effectively by a conventional passive EMI filter. However, the image of the sensed noise (injected noise) is gradually distorted as the frequency increases due to the effect of the frequency on the opamp characteristic. This signal distortion has a direct impact on the performance of the filter at higher frequencies. This limitation requires the necessity of the passive EMI filter to be employed, since this latter has a good performance at higher frequencies with the advantage of reducing the size of its passive components.

2.4 Output active EMI filters versus combined active and passive EMI filters

Output active EMI filters have been proposed (Mingjuan et al., 2005; Lee et al., 1996). They are based on the process of injecting 180 degrees out of phase image of the output voltage ripple or output current ripple back to the output DC rail. However, these approaches require a bigger inductor size to carry the DC output current which is not a

feasible solution for many power applications since it generates current losses and degrade the total power efficiency of the converter. In addition, placing the filter circuit at the output of the DC/DC converter, will introduce an additional pole in the control loop of DC/DC converter. This can jeopardize the stability of the converter under different load conditions. Furthermore, most of the previous work has been centered on the differential-mode noise attenuation rather than the common-mode (CM) noise attenuation which forms the dominant part of the conducted noise source in DC/DC converters. The separation of the CM and DM noise at the input of DC/DC converters has been developed and dealt with in (Guo et al., 1996). It has been clearly demonstrated that to improve the passive EMI filter performance (noise attenuation), it is important to know which dominant-mode noise that needs to be suppressed.

To overcome the limitations that are inherent in the existing work, we propose, in this master thesis, a combination of an active EMI filter and a passive filter that is aimed to attenuate the common mode conducted noise. The combined active and passive filter is placed in the input side of DC/DC converter so that the inductor element can be exposed to a minimum DC current, which can be reflected in a significant reduction of the size of the passive filter and less power losses that are generated inside the magnetic core of the filter inductor, hence improving the overall efficiency of the DC/DC converter. In addition, placing the passive filter at the input of the DC/DC converter will not interfere with the control loop stability of the DC/DC converter which makes this configuration compatible with any DC/DC converter topology.

In this approach, the attenuation of the EMI noise can be achieved by both the active and the passive filter circuits. First the active circuit samples the noise source, inverts the sampled noise in order to replicate the noise signal with 180 degrees phase-shift and finally, injecting the inverted signal back to the input of the DC/DC converter for the noise cancellation to take place. The residual noise that can not be attenuated by the active circuit will be pickup by the passive circuit to obtain an optimum attenuation across the EMC frequency spectrum (150 KHz -30 MHz). The novelty of this filtering method can be described in two folds; first, it improves the existing passive filter in terms of size, cost and thermal losses, second, it provides better overall performance on the reduction of the conducted EMI noise that will be demonstrated in later chapters. The next section presents the developing trends of the EMI filters.

2.5 Conclusion

In this chapter, some EMI mitigation techniques, using passive and active filtering, have been presented. Different configurations of passive filter have been introduced. Some design considerations including the effects of the mismatch impedance on the insertion loss of the filter, components selection and the stability are presented as well. In addition, an active EMI filter has been introduced. The operation as well as the circuit elements has been described. The performance limitations of the active EMI filter, at high frequency, have been discussed. Some active filters circuit configurations have been presented. Finally, given the limitations of the output EMI active filter, the selection of the combined input active and passive EMI filter is proposed. In the following chapter,

detailed circuit description and analysis will be discussed and experimental results to prove the feasibility and the viability of the proposed approach will be demonstrated.

Chapter 3

Active and passive input EMI filters for DC-DC converters

3.1 Introduction

The previous chapter presented the different circuit configurations of the passive EMI filter. It also, provides criteria such as, the input and load impedances that should be taken into account when designing a proper passive EMI filter. It mentioned the drawbacks of the passive EMI filter, in terms of thermal losses, size and cost. The active EMI filter has also been introduced as an alternative solution to the limitations of the passive EMI filter performance at low frequency. Hence the reduction of the size, cost and minimum thermal losses have been achieved. In this chapter, a combined active and passive EMI filter has been proposed and has been submitted (October 2006) as a publication paper to the IEEE transaction on industrial electronics (Hamza et al., 2006). The novelty resides in the EMI filtering method using both active and passive circuitry at the input of the DC/DC converter, to achieve optimum common-mode noise attenuations at low and high frequency, and significantly reducing the size and minimizing the losses that are generated in the passive filter circuit, due to operating current.

The paper introduces the importance of the EMI attenuation, in particular, the conducted noise emissions which act as disturbance to the proper functioning of the DC power distribution. Some literatures dealing with EMI filtering methods have been mentioned.

The operating principles of the proposed EMI filter have been described. The basic elements of the active EMI filter have been explained. A design example is provided to demonstrate the validity of the proposed EMI filter. The experimental results of the proposed EMI filter as well as the test setup have been presented at the end of the paper. The last section of the paper concisely elaborate on the performance achieved using the proposed filtering method.

3.2 CONDUCTED NOISE MITIGATION IN DC-DC CONVERTERS USING ACTIVE FILTERING METHOD

Djilali Hamza, P.Eng, and Mohamad Sawan, Fellow, IEEE

Department of Electrical Engineering, École Polytechnique de Montréal

Montréal, Québec, Canada, H3C3A7

djilali.hamza@polymtl.ca

Abstract - Electromagnetic Interference (EMI) noise mitigation is an important issue that should be addressed and emphasized when designing DC/DC converters. These later, are known to be the primary culprit of the EMI noise generation in most of the electronic systems, mainly due to the switching action of the MOSFET circuitries. The noise coupling between the positive supply bus and ground is the predominant factor of the total conductive noise generated in DC/DC Converters. This noise type is referred as

Common Mode (CM) noise. A portion of this noise is converted into Differential Mode (DM) type which has a path between the positive bus and its return.

Passive LC filters have been the intuitive solution for EMI noise mitigation; hence they have been included in most of the DC/DC converters. However, their size, weight and cost can cause a significant constraint in some applications. To overcome these constraints, an active EMI filter is proposed. The active filter is based on the image of the noise current phase shifted by 180 degrees and injected back to the DC bus. The combination of the active and the passive filters shows a substantial attenuation of the conducted emissions as compared to the passive filter only. Also, this combination contributes to the reduction of the size and weight of the passive filter. Experimental results to demonstrate the performance and the effectiveness of the active EMI filter in DC/DC converters are presented.

Key Words: EMI, EMC, Passive filter, Active filter, DC/DC converter, Common-Mode noise, Differential-Mode noise.

3.3 Introduction

While DC/DC converters are well known for their significant advance in their power density per square inch, and their low thermal dissipation, the thread of generating Electromagnetic Interference (EMI) noise from the high frequencies embedded in their fast switching di/dt and dv/dt has always been a concern. As the DC/DC converters follow the new trend of power generation, their switching frequencies have increased

dramatically to reduce their dimensions. Most of these DC/DC converters are PCB mount type and are installed in close proximity to microprocessors or to provide DC supply to motherboards. Thus, having a DC/DC converter that can coexist with microprocessors without disturbing their operation could be a challenging design. The process of having the DC/DC converter to comply with its own environment, in terms of EMI, is referred as electromagnetic compatibility (EMC). This becomes an integrated part of the design requirements that should be addressed at the early stage of the project. Further details on EMI generation in power electronic converters can be found in [1].

The EMI noise can be radiated in free space or conducted through power leads. However in this paper, only conducted noise will be discussed. There are two different modes of conducted noise, common mode (CM) and differential mode (DM) conducted EMI. These noise modes are thoroughly detailed in [2]. Conducted EMI noise can be attenuated by placing a high impedance in series and low impedance in parallel with the input DC bus. This can be achieved by using LC passive components. This method is known as LC passive filtering. As reported in [2], it is important to discern between CM and DM noises to design a suitable passive filter. There are other criteria that can be taken into account, when designing passive filters such as input and output impedances with respect to the input impedance of the DC/DC converter. These are described in [3]. Depending on the application and the environment in which the DC/DC converter will be installed, the EMC standard limits might be relaxed or very stringent. In some cases LC filter can not achieve the required noise attenuation to bring the noise signature below the

limits. Multi stage LC filters could be used. However this solution will result in an extended size of the DC converter. As an alternative, a combination of an active filter with one stage LC filter, as shown in Fig. 1, would yield an optimum attenuation. This configuration, which is also known as hybrid filter, results in less components count, smaller size, less weight and lower thermal dissipation. The milestone is a DC/DC converter that complies with EMC standard class-A limits [4]-[5].

Figure 3.1

In Fig. 3.1, several combinations of active and passive filters have been shown. These combinations can be configured at the input of the DC/DC converter for input noise/ripple current attenuation or at the output of the DC/DC converter for the output noise/ripple voltage attenuation.

So far, a few schemes of the combination of an active filter with one stage LC filter (hybrid filter) have been proposed [6]-[7]. They are based on the process of injecting 180 degrees out of phase image of the output voltage ripple [8]-[9] or output current ripple back to the output DC rail. However, these approaches require a bigger inductor size to carry the DC output current which is not a feasible solution for many power applications. In addition, placing the filter circuit at the output of the DC/DC converter, will introduce an additional pole in some converters topologies, which can jeopardize the DC/DC converter stability. Furthermore, most of the previous circuits have been centered on the differential-mode noise/ripple attenuation rather than the common-mode (CM) noise

attenuation which forms the biggest part of the conducted noise source in DC/DC converters [11].

Since the transmission of the common-mode noise, which is entirely done through parasitic or stray capacitors and stray electric and magnetic fields, becomes very significant, due to very high switching frequency. The noise appearing on the ground line contributes significantly to the EMI. Therefore, we propose in this paper to explore the combination of the active and passive filters in terms of common mode conducted noise attenuation. The combined active and passive filter is placed on the input side of DC/DC converter so that the inductor element can be exposed to less DC current and can not interfere with the stability of the DC/DC converter. The filter can sense, invert, and inject the noise signature back to the input bus of the DC/DC converter.

In section 3.4 of this paper, the circuit description and analysis of the proposed hybrid filter configuration is presented. Section 3.5 illustrates the design consideration of the proposed active input EMI filter, including the selection of an operational amplifier (opamp) circuitry and the design of the transformer based voltage injector. Section 3.7 describes the experiment of the proposed filter combination to the input of a DC/DC converter, and compares its performance to that of LC passive filter only. Finally, some conclusions are drawn in section 3.8.

3.4 Description of the proposed filter combination

3.4.1 Circuit description

The proposed hybrid filter consists of an active filter and one-stage passive filter as shown in Fig. 3.2. L_{in} and C_{in} form the input passive filter. The active filter consists of the sensing branch C_s and R_s, the opamp block or the active device, and the transformer based voltage injector.

Figure 3.2

In this work, the input ripple and noise current is sensed through a RC branch circuit. This type of sensor is simple and efficient for sensing only the ac-signal while rejecting the DC one. There are other methods of sensing the input current noise using a wide-band transformer as detailed in [10]; however, this method requires a larger magnetic core to ovoid saturation, in particular when it is placed at output of the DC/DC converter. The ripple voltage which is in the phase of the input ripple current is fed into an inverting opamp to inverse the phase of the sensed noise signal. The output signal of the opamp is injected back into the converter through a transformer with the desired gain. Then this injected voltage is converted into current through the shunt inductor which is part of the passive filter elements. Based on the superposition theorem of signals with equal amplitude and opposite phase, the injected ripple current should cancel out the incident input ripple current.

3.4.2 Circuit analysis

Consider a DC/DC converter with Z_{in} being the input impedance and I_n being the ripple current that is generated by the switching elements. The equivalent circuit model of harmonic noise of the DC/DC converter with only the passive filter and the converter with the hybrid filter proposed in Fig. 3.2 are shown in Fig. 3.3(a) and Fig. 3.3(b) respectively.

Figure 3.3

Assume that the current that is injected into the utility mains in Fig. 3.3(a) and Fig. 3.3(b) is I_{in} and I'_{in} respectively, the performance (figure of merit) of the active filter can be evaluated by its noise attenuation defined as:

$$FM = \frac{I'_{in}}{I_{in}} \tag{3.1}$$

where I_{in} and I'_{in} are the noise currents that are injected into the mains by the DC/DC converter with passive filter only and with the hybrid filter respectively.

In the frequency domain, the current I_{in} and I'_{in} can be derived according to Fig. 3.3:

$$I_{in} = I_n \cdot \frac{1}{1 + sC_{in}(Z_{in} + sL_{in})} \tag{3.2}$$

$$I'_{in} = I_n \cdot \frac{R_s \cdot \frac{1}{E} \cdot \frac{1}{sC_{in}} + \frac{1}{sC_s} \cdot \frac{D}{sC_{in}E}}{Z_{in} + R_s\left(1 - \frac{R_s(1 + A_v N)}{E}\right) + \frac{1}{sC_s}(1 + F \cdot D)} \tag{3.3}$$

where L_{in} and C_{in} are inductor and capacitor components of the input passive filter

R_s and C_s are the resistive and capacitive components of the sense circuit N is the gain of the injection transformer

$$D = \frac{1}{sL_{in} + \frac{1}{sC_s}} \tag{3.4}$$

$$E = R_s(1 + A_v N) + \frac{1}{sC_{in}} \tag{3.5}$$

$$F = -\frac{1}{sC_s} - A_v N R_s \left(\frac{R_s(1 + A_v N)}{E} - 1 \right) \tag{3.6}$$

and A_v is the closed-loop voltage gain for an inverting opamp with unity gain that includes the frequency-dependant open-loop gain function A(s):

$$A_v = \frac{-A(s)}{2 + A(s)} \tag{3.7}$$

$$A(s) = \frac{k_1}{1 + s/k_2} \tag{3.8}$$

where k_1 is the DC open-loop voltage gain (typically 10^5 to 10^7), and k_2 reflect the cutoff frequency. These two parameters describe the frequency-dependant open loop characteristics of the chosen opamp.

Therefore, the noise attenuation of the proposed circuit can be found by substituting I_{in} and I'_{in} in equation (3.1) by equations (3.2) and (3.3) respectively, and plotted in frequency domain as shown in Fig. 3.4.

Figure 3.4

It can be seen that, in the frequency range of interest (150 kHz-30 MHz), the proposed active filter has substantial noise attenuation, also referred as insertion loss of 30 dB at the fundamental switching frequency in the range of a few hundreds kHz, and around 20 dB at the first several harmonics. It is also found that the noise attenuation is not only

dependant on the characteristics of the opamp (k_1 and k_2), but also highly dependent on the value of the shunt inductor L_{in}. In Fig. 3.4, the smaller value of L_{in} results in better noise attenuation. However the minimum value of L_{in} should be limited by the cut-off frequency of the input passive filter, which should be set at a decade lower than the resonant frequency of the output filter of the DC/DC converter to avoid interaction between the two.

3.5 Design consideration of the proposed active EMI filter

The main elements of the proposed active EMI filter, as shown in Fig. 3.2, are the sensing elements R_s and C_s, the op-amp circuit or the active control unit, and the transformer based voltage injector. Design and selection of each element are addressed in the following sub-sections. Accordingly, one design example is given at the end of this section.

3.5.1 Sensing Elements

To ovoid interaction between the sensing RC branch and the input/output filters, it is important that the cut-off frequency of the high pass RC branch filter be placed well below the switching frequency of the DC/DC converter. The design of the RC branch follows the conventional high-pass RC filter design procedures and the cut-off frequency is placed at a factor of 100 below the ripple signal fundamental switching frequency.

3.5.2 Active controller

In theory, by placing an active filter in the DC/DC converter circuit, the resultant input ripple current would be reduced to zero if the opamp was ideal. However, in practice, the

bandwidth of the opamp limits the performance of the active filter. In Fig. 3.2, the opamp is used at unity gain to maintain its maximum bandwidth and the desired gain of the active filter can be achieved by the injection transformer.

However, depending on the type of the opamp selected for the application, there is always a minimum phase error and distortion of the input signal at very high frequencies due to the parasitic elements inherent in the opamp itself. Fig. 3.5 Shows the input and output signals of an AD8004 opamp when it is used as a voltage follower at two different operating frequencies. It can be seen that the phase error and distortion are negligible at 700 KHz, but become significant at 10MHz.

Figure 3.5

Fortunately, the bandwidth of the opamp does not need to cover the whole EMI spectrum since the noise current spectrum generally falls off at 40dB/dec at higher frequencies. Therefore, it is sufficient to select an opamp whose gain-bandwidth is high enough to provide good noise attenuation for the first several harmonics of the switching frequency, the rest of the harmonics will be taken care of by the passive filter.

3.5.3 Transformer based injector

A transformer based injector is used in this design. This could be accomplished by using a high frequency transformer with parallel inductor on the secondary windings. As shown in Fig. 3.2, the passive filter element L_{in} is used as the shunt inductor to handle the DC current flown through the secondary power circuit, and meanwhile, convert the injected voltage noise into a current form. Both, the injection transformer and the shunt inductor,

should provide sufficient impedance to ovoid loading the opamp. It is important that the injection transformer replicates the injected signal with high precision, and its turn ratio can be derived as follows.

As seen in Fig. 3.2, the voltage at the primary winding of the injection transformer is equal to the voltage noise at the output of the active filter. The injected voltage noise at the secondary winding generates the injected current noise through L_{in}. Accordingly; three basic equations can be established:

$$N = \frac{v_{it\_1}}{v_{it\_2}} = \frac{v_{op}}{v_{it\_2}} \tag{3.9}$$

$$v_{op} = R_s i_{rn} \tag{3.10}$$

$$i_{inj} = \frac{v_{it\_2}}{n\omega_s L_{in}} \tag{3.11}$$

Where v_{it_1} and v_{it_2} are the voltages at the primary and secondary windings of the injection transformer; v_{op} is the output voltage of the opamp; R_s is the resistance of the sensing element; ω_s is the switching frequency; i_{rn} is the input ripple current; i_{inj} is the injected current noise; and n is the order of the harmonic component. Ideally, the injected current noise should cancel the input ripple current:

$$i_{inj} + i_{rn} = 0 \tag{3.12}$$

It can be seen that at different harmonic frequencies, different transformer turn ratios are required to cancel the corresponding harmonic component precisely. In order to cancel the dominant harmonic noise to maximize the attenuation performance of the active filter,

the transformer turn ratio should be derived at switching frequency (n=1). Rearranging the above equations, the transformer turn ratio can be found as:

$$N = \frac{R_s}{\omega_s L_{in}} \tag{3.13}$$

3.6 Design example

A 30W DC/DC isolated forward step-down converter operating at 700 KHz switching frequency is taken as a design example. The input nominal DC voltage is 28V, and the out voltage is regulated at 5V. An active filter is placed between the input voltage source and the input passive filter as shown in Fig. 3.2. The circuit parameters of the active and passive filters are selected according to analysis given in sections 3.2 and 3.3, and are illustrated as follows.

3.6.1 Passive filter

As seen from Fig. 3.4, with L_{in} =1 μH the hybrid filter provides a good attenuation around 30dB at switching frequency of 700 kHz, and around 20dB at its 2nd and 3rd harmonics, corresponding to the frequency of 1.4 MHz and 2.1 MHz respectively. If the cut-off frequency of the passive filter, namely $f_{c\_passive}$, is set at 40 kHz, the value of C_{in} can be found as:

$$C_{in} = \frac{1}{(2\pi f_{c\_passive})^2 L_{in}} = 20\mu F \tag{3.14}$$

3.6.2 Sensing elements

If the cut-off frequency of the sensing high-pass RC branch, namely f_{c_s}, is set at 7 kHz, and assume that the sensing resistance R_s is equal to 50Ω, the value of C_s can be found as:

$$C_s = \frac{1}{2\pi f_{c\_s} R_s} = 3\mu F \tag{3.15}$$

3.6.3 Active controller opamp

This selection of the opamp is highly dependent on the switching frequency of the DC/DC converter. A wideband opamp is selected to cover the conducted emission frequency spectrum which extends from 150 KHz to 30MHz according to EN55022 standards. AD8004 current feedback amplifier is sought to be suitable for this application with its bandwidth of 250MHz at unity gain, more than 200 times greater than that of the all purpose amplifier UA741. Other features of the AD8004 are very high slew rate up to 3000V/us and high output current of 50mA.

3.6.4 Transformer based injector

The turn ratio of the injection transformer is calculated according to equation (3.13) and can be found as N=11.

3.7 Experimental results

The prototype circuit is a 30W DC/DC isolated forward converter operating at 700 KHz switching frequency, the input current of the converter is set at 1A and the output voltage is controlled at 5VDC using pulse width modulation (PWM) technique. The nominal input voltage is set at 28VDC. Circuit diagram of the converter prototype along with the

passive and active input EMI filters is shown in Fig 3.6. The circuit parameters are selected based on the design example discussed in section 3.4.

Figure 3.6

Tests were done according to EMC standards EN55011 (CISPR 11) [4] and EN55022 [5] test setup for conducted emissions. The test setup diagram is shown in figure 3.7.

Fig. 3.7

In both figures 3.6 and 3.7, the Line Impedance Stabilization Network (LISN) is connected at the input of the DC/DC converter as the sensing element and represents a known common mode impedance of 50 Ω. The LISN is well known to establish a standard profile of load impedance toward the EMI source and also, filter out the high frequency disturbances on the mains that could create measurements uncertainties. A spectrum analyzer was used to display the input noise/ripple signature in frequency domain, ranging from 150 KHz to 30 MHz as stated in the EN55022 standards. The noise/ripple voltage was measured across the 50 Ω LISN which is connected to the spectrum analyzer with a shielded cable. Results are displayed in dBuV versus frequency as per EMC standards.

First measurements were conducted with the active EMI filter removed from the prototype DC/DC converter. However, the passive filter remained connected at the input of the converter. The result of the EMI noise voltage is shown in Fig. 3.8. Dominant peaks can be seen at the fundamental switching frequency (700 kHz) and at other harmonics. However, good harmonics attenuation is achieved at higher frequencies. This

is due to the contribution of the passive filter since this latter provides 40 dB attenuation beyond its cut-off frequency.

Another set of measurements were taken with the active EMI filter inserted between the LISN and the passive filter. The corresponding result of the EMI noise spectrum, as per EN55022 standards, is shown in Fig. 3.9.As it can be seen, significant noise attenuation is achieved at the fundamental switching frequency and at the first harmonics. This is due to the contribution of the active filter. Table 3.1, compares the peaks attenuation accomplished by the passive and the hybrid filters.

Figure 3.8

An attenuation exceeding 30 dBuV is observed at the switching frequency and at the first higher harmonics. These attenuation magnitudes make a significant difference in the EMC compliance in terms of conducted emissions.

Figure 3.9

The active filter has less performance for the attenuation of the higher frequency noise due to the following two main reasons: (1) The injection gain of the active filter is dependent on the transformer based injector, whose turn ratio is designed based on the switching frequency; and (2) The opamp used in the active filter generates more phase-shift for the harmonics at higher frequency as shown in Fig. 3.5. Therefore, the active filter adds more contribution, in terms of noise attenuation, on the fundamental and on the first several switching harmonics. In this way, the active filter can significantly reduce the size of the passive filter whose cut-off frequency can be set at much higher frequency.

3.8 Conclusion

The combination of the input EMI active and passive filters in DC/DC converters has produced improved performance in the input EMI noise mitigation. As demonstrated in this paper, active filter has a significant impact on attenuating noise signals at the fundamental switching frequency and the first harmonics. However, this type of filters has proven to be less affective at higher frequency noise (above 10 MHz). In such a case, the passive filter with properly designed cutoff frequency can be used to attenuate higher frequency EMI noise signals. In application such as transponders of a satellite payload, where conducted noise emissions requirements are stringent, active input EMI filter combined with passive EMI filter provides a viable solution.

3.9 References

[1] Laszlo T. "Electromagnetic Compatibility in Power Electronics" IEEE Press, New York, 1995.

[2] Ting G., Dan Y. C., Fred C. Lee, "Separation of the Common-mode and Differential-mode conducted EMI noise" IEEE Transactions on Power Electronics, Vol.11, No.3, pp. 480 -488, May 1996.

[3] Martin F.L., Arthur F.W., "Input filter Design for multiple-module DC power systems" IEEE Transactions on Power Electronics, Vol.11, No.3, pp. 472 - 488, May 1996.

[4] EN55011 Limits and methods of measurement of radio disturbance characteristics of industrial, scientific and medical (ISM) radio frequency equipment, pp. 12 - 87, 1999-08

[5] EN55022 (CISPR22) Information Technology Equipment (ITE) – Radio disturbance characteristics – Limits and methods of measurement, pp. 10 - 62, February 1995

[6] LaWhite, L.E., and Schlecht, M.F, "Design of active ripple filters for power circuits operating in the 1-10MHz range" IEEE Transactions on Power Electronics, Vol 3, No 3, pp. 310 -317, 1988.

[7] Farkas, T., and Schlecht, M.F., "Viability of active EMI filters for utility applications" IEEE Transactions on Power Electronics, Vol. 9, No. 3, pp. 328-337, May 1994.

[8] D.Y. Lee, B.H. Cho, "Design of an input filter for power factor correction (PFC) AC to DC converters employing an active ripple cancellation" Energy Conversion Engineering Conference. Proceedings of the 31st Intersociety, Vol.1, pp. 582 – 586, 1996.

[9] Mingjuan Z. and David J. P., "Design and Evaluation of feedforward Active Ripple Filters" IEEE Transactions on Power Electronics, Vol. 20, No. 2, pp. 276 - 285 March 2005.

[10] Yuk, K.W., and Yim-Shu, L. and David, K.C, "Synthesis of a wide bandwidth current sensor using a current transformer for active power filter applications" IEEE- PESC, Vol.1, pp. 270 – 273, 2000.

[11] JUNICHI, M., MASAYUKI, M., "Measurement of the Source Impedance of Conducted Emission Using Mode Separable LISN" Electrical Engineering in Japan, Vol. 139, No, 2, pp. 1376-1381, 2002

3.10 List of figures

3.11 List of tables

3.12 Figures

Erreur ! Liaison incorrecte.

Figure 3.1 Two combinations of active and passive filtering schemes: (a) Filtering at the input side of the DC/DC converter; (b) filtering at the output side of the DC/DC converter

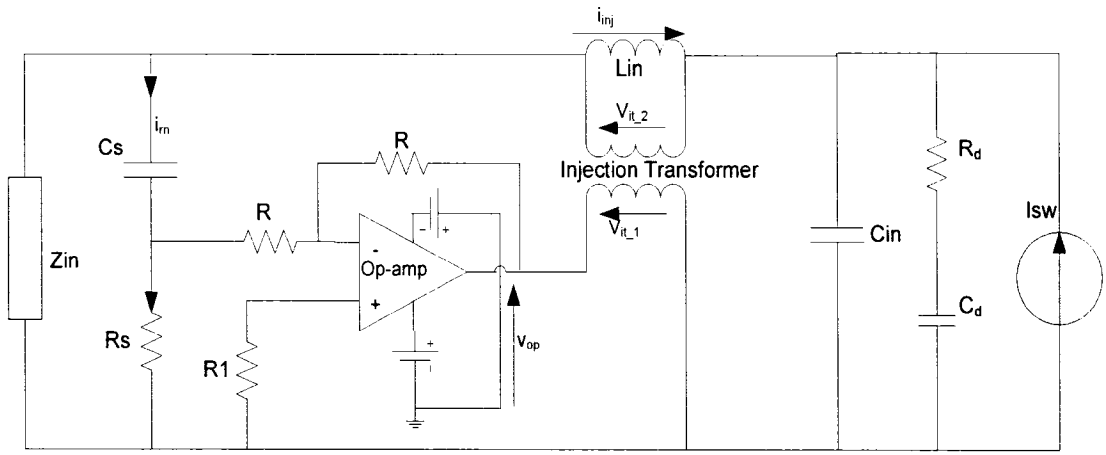

Figure 3.2 The configuration of the proposed hybrid filter

Erreur ! Liaison incorrecte.

Figure 3.3 Equivalent harmonic circuit of the converter: (a) Equivalent circuit with passive filter only, (b) Equivalent circuit with hybrid active and passive filters

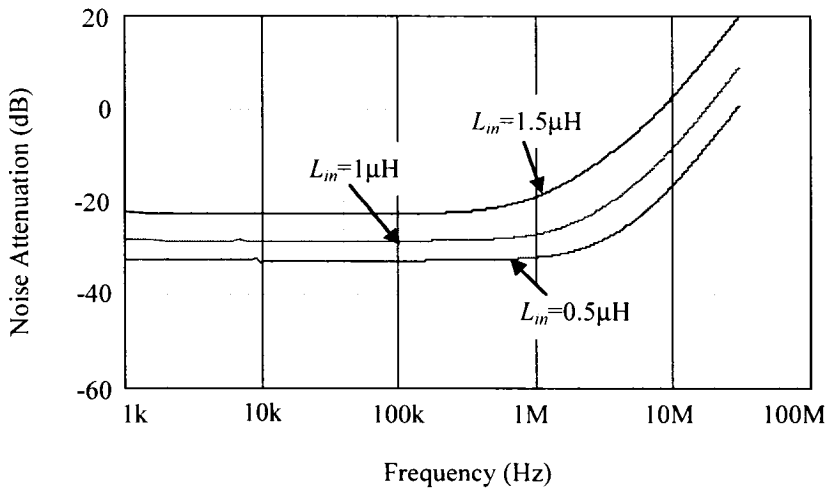

Figure 3.4 Noise attenuation of the proposed circuit (Z_{in}=50Ω//50μH, R_s=50Ω, C_s=5μF, C_{in}=20μF, k_1=6·10^6, k_2=100, N=15)

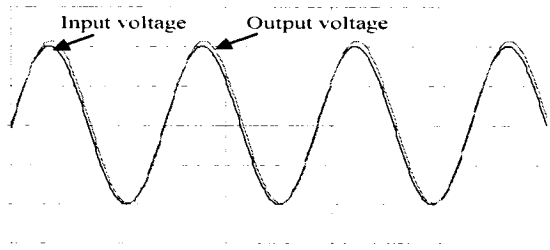

(Scales: Horizontal: 0.1μs/div; Vertical: 50mV/div)
(a)

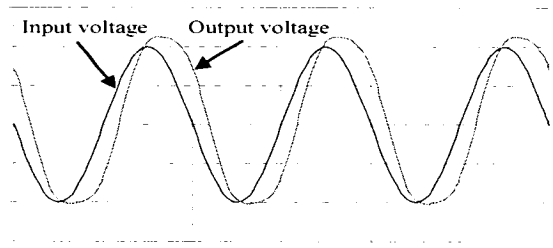

(Scales: Horizontal: 0.05μs/div; Vertical: 50mV/div)
(b)

Figure 3.5 Phase error and distortion of op-amp at two different operating frequencies: (a) Phase error at 700 KHz, (b) Phase error at 10 MHz

Erreur ! Liaison incorrecte.

Figure 3.6 Experimental circuit diagram

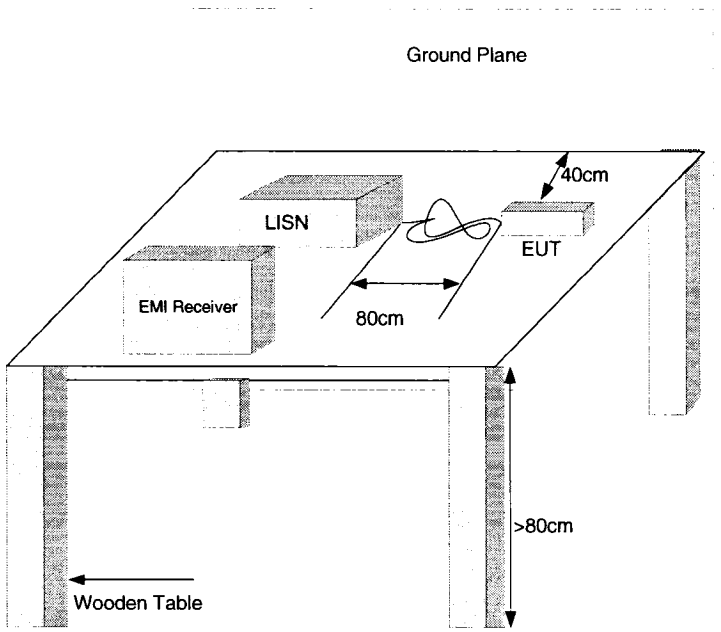

Figure 3.7 Experimental test setup diagram

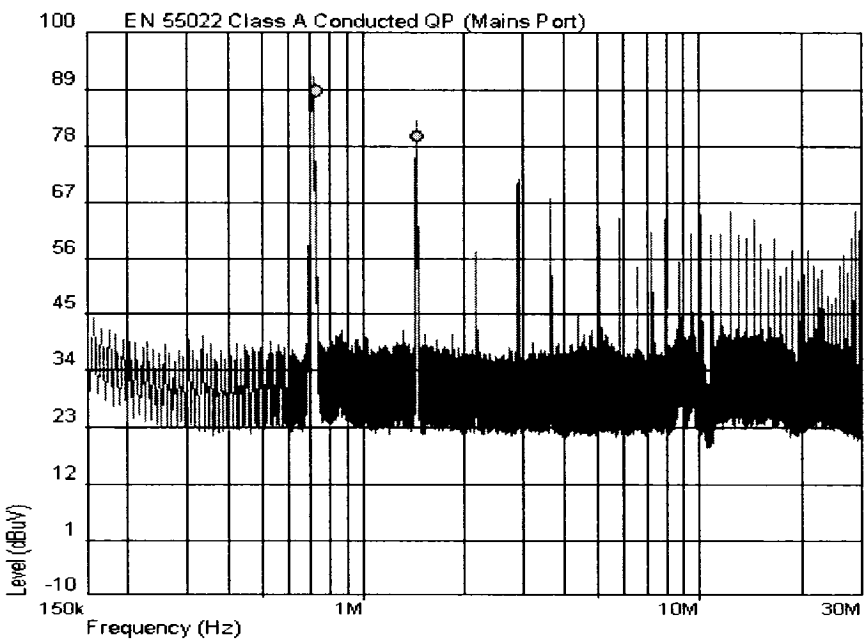

Figure 3.8 Conducted EMI noise spectrum result with the passive filter only

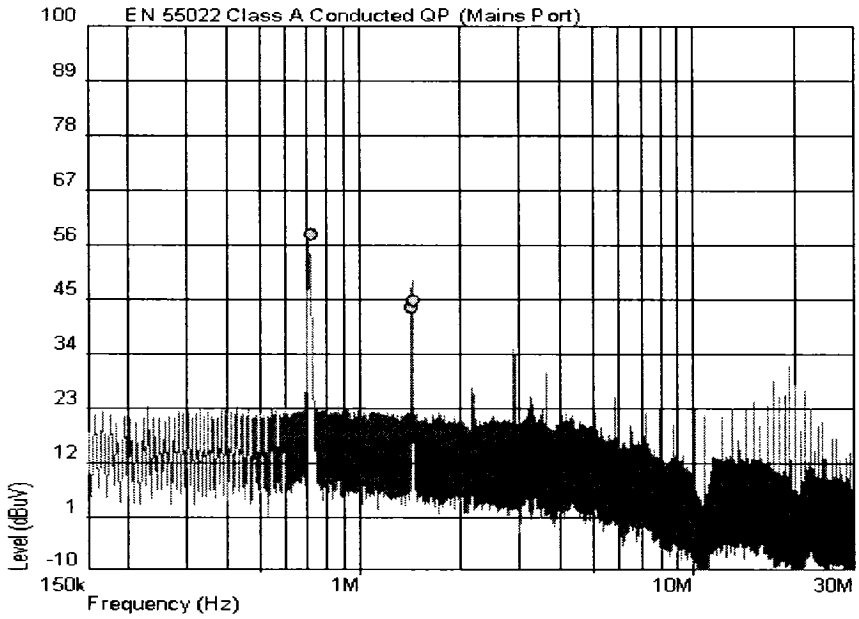

Figure 3.9 Conducted EMI noise spectrum result with the combination of passive and active filters

3.13 Tables

Table 3.1 Performance comparison of the passive and the hybrid filters

Harmonic Frequency (MHz)	Peaks magnitude With passive filter (dBuV)	Peaks magnitude With hybrid filter (dBuV)	Delta attenuation (dBuV)
0.7	88.9	57.9	31
1.4	79.9	43.4	36.5
2.1	57.2	27.4	29.8
2.8	70.6	35.3	35.3
3.6	67.7	30.3	37.4

Chapter 4

Simulation and Complimentary Experimental Results

This chapter provides a detailed explanation on the measurements method and the test setup used for the proposed EMI filter prototype. These measurements are briefly mentioned in chapter 3 which is the journal publication. Simulation and experimental results will be commented and compared.

4.1 DC/DC converter Platform

A DC/DC converter prototype was designed and built to be used as a platform for the active EMI filter evaluation. The converter represents the EMI noise source to the filter and uses UC2843 Pulse Width Modulation (PWM) controller to keep the output constant at all load variations. A switching frequency of 700 KHz has been selected to minimize the magnetic size. A forward topology is used for this prototype which operates from a 28Vdc input bus and has an output voltage and current of 5VDC and 1A respectively. Further details on the design calculations of the DC/DC converter using MathCAD software, can be found in Annex A at the end of this document. Figure 4.1 shows a simplified block diagram of the active EMI filter connected to the DC/DC converter. A photo snapshot of the DC/DC converter including the active EMI filter prototype is shown in Figure 4.2

In terms of circuit simulation, a complete forward DC/DC converter circuit including the active EMI filter was simulated using PSPICE CAD software. The schematic diagram along with the circuit layout and the list of the components can be found in Annex B of this document.

Erreur ! Liaison incorrecte.**Figure 4.1 Simplified block diagram of DC/DC converter with the active EMI filter**

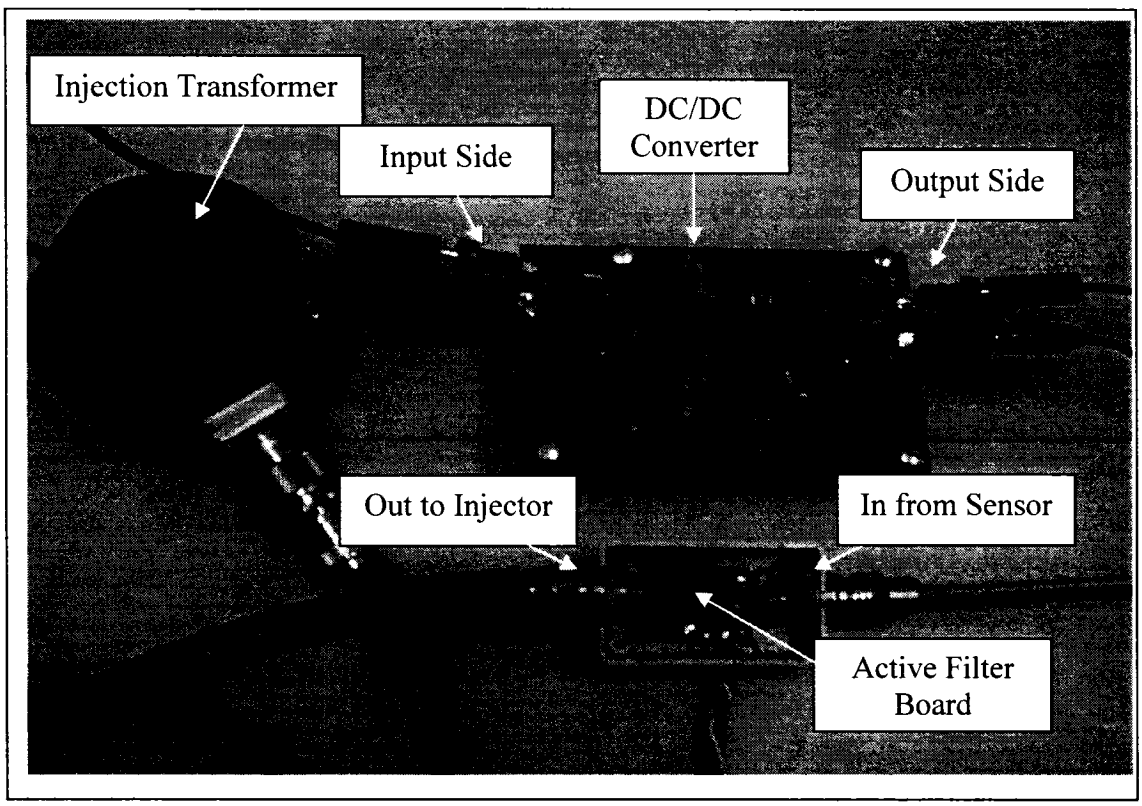

Figure 4.2 Photography of the DC/DC Prototype with proposed active EMI filter

4.2 Test setup

All the data acquisitions for the conducted emissions testing were taken using the setup shown in Figure 4.3. The measurements were taken according to the limits for conducted

disturbance at the power ports of the CISPR 22 class A standard. These limits are shown in Table 4.1 below. The conducted noise voltage generated by the DC/DC converter, is sensed from the sense port of the line impedance stabilization network (LISN) then it is fed through the active EMI filter circuit. The output of the active filter is connected to an injection transformer which is used to inject the noise signal back to the input lead of the DC/DC converter to cancel out the input noise. The input and the output noise signal of the active EMI filter is displayed in both frequency and time domain using spectrum analyzer and oscilloscope respectively.

Erreur ! Liaison incorrecte.

Figure 4.3 Test setup diagram for the active filter conducted noise measurements

Table 4.1 CISPR 22 limits for conducted disturbance at mains ports Class A

Frequency Range (MHz)	**EMC Limits (dBuV)**	
	Quasi-peak	**Average**
0.15 to 0.50	79	66
0.5 to 30	73	60

4.3 Simulation results

To compare the simulated to the experimental results, an entire DC/DC converter including an LC passive EMI filter circuit, was simulated in PSPICE software. Most of

the components models exist in the software library, except the LISN which was modeled to represent 50Ω utility source impedance. The primary (input) current signature is simulated by the current controlled current source (CCCS) which can be flown through the LISN sense branch (RC high-pass filter) to generate the corresponding noise voltage. Complete simulated circuit diagram as well as the PSPICE source code can be found in Appendix C at the end of this document.

The simulation is run in two steps, both of which the transient analysis mode was used with a stop-time and step-size of 500us and 100ns respectively. In the first step, the simulation was run with only the passive LC filter connected to the DC/DC converter, and then the active EMI filter was added to the converter circuit to observe the overall contribution in terms of input noise attenuation. In both simulation cases, a Fast Fourier Transform (FFT) was performed on the sensed voltage at the LISN sense port in order to represent the noise voltage in terms of its harmonic contents in the frequency domain. Waveform showing the simulated conducted EMI noise spectrum without the active filter and with the active filter installed in the circuit is depicted in Figure 4.4 and Figure 4.5 respectively. As it can be seen from these figures, that the EMI noise is attenuated by about 30 to 40 dB, when the active filter is used in the circuit. Notice that the peak at the fundamental frequency (700 KHz) is attenuated by approximately 35 dB. The first few harmonic peaks are labeled on the plot along with their corresponding frequencies.

4.4 Comparison between the simulation and experimental results

Table 4.2, compares the EMI noise peaks in the frequency domain, of the simulated circuit to the experimental prototype circuit with the active EMI filter connected to the DC/DC converter. Some discrepancies are observed on the simulated results as compared to the experimental results which mainly due to the software limitation in the components modeling. However, overall signature of the simulated EMI noise revealed to be similar to the experimental noise results obtained from the spectrum analyzer. In this regard, the conducted EMI noise can be quantified using simulation software as a tool in the post layout design and evaluation of the EMI filter.

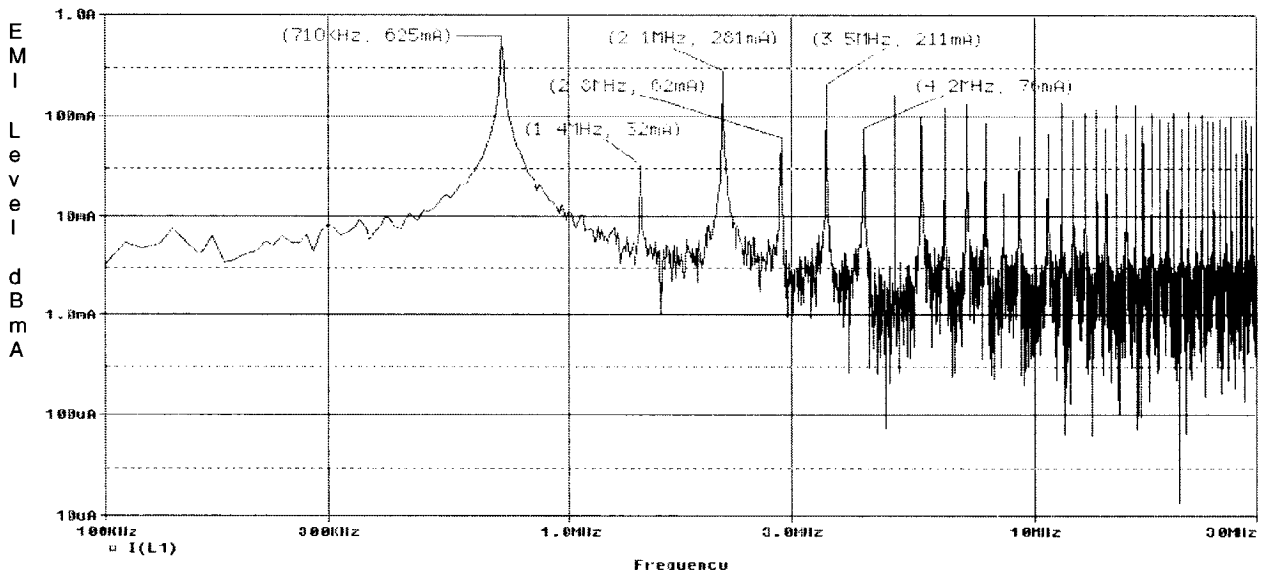

Figure 4.4 Conducted EMI noise spectrum with no filter installed (Simulation)

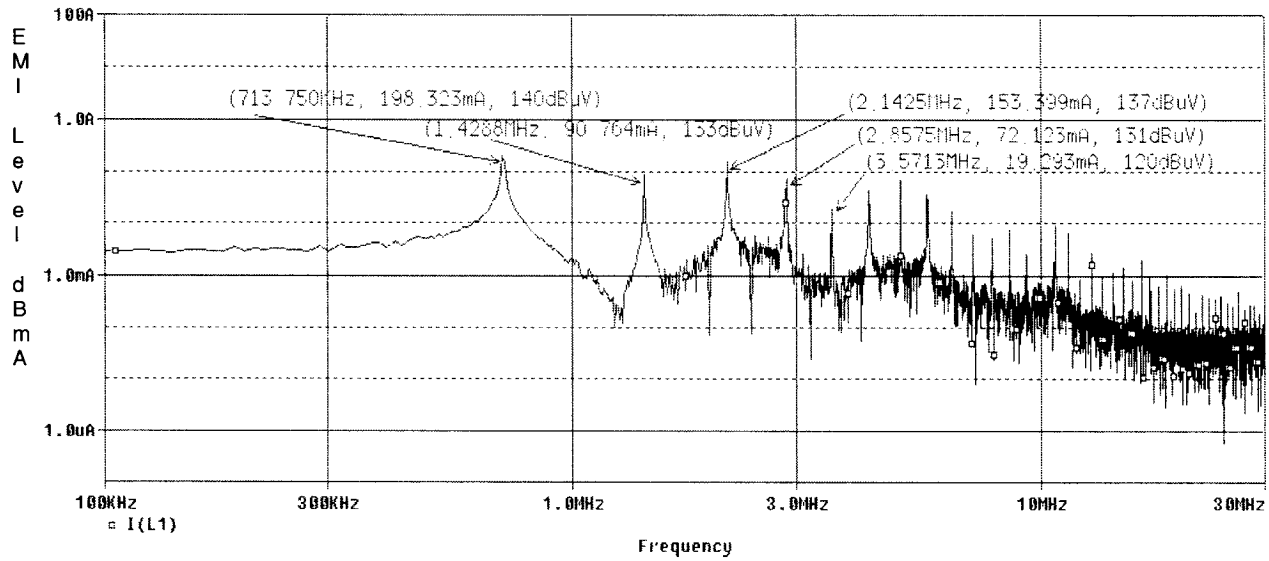

Figure 4.5 Conducted EMI noise spectrum with passive filter (Simulation)

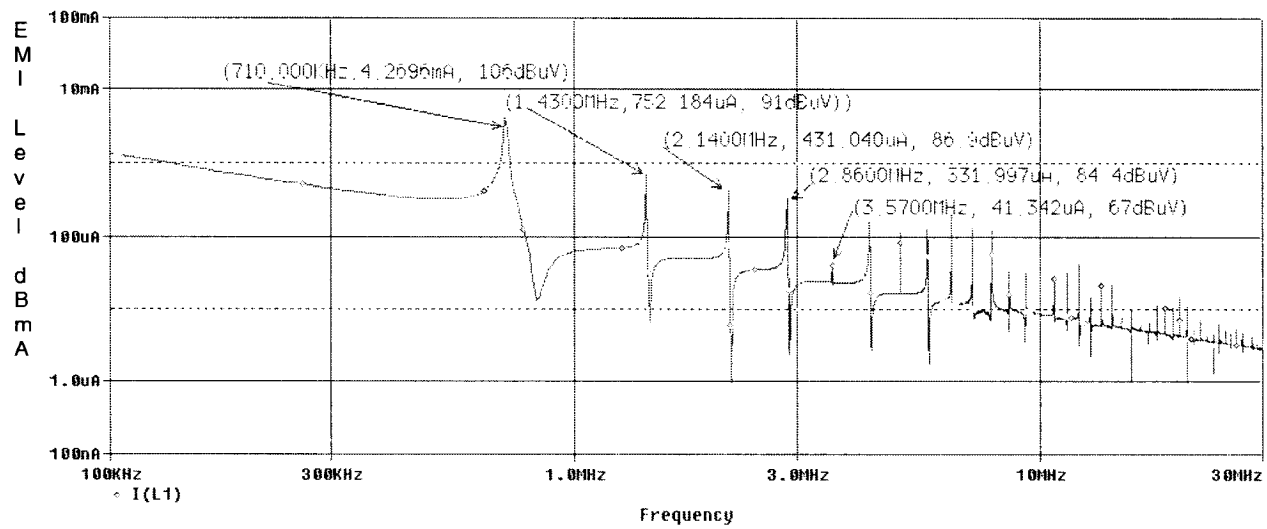

Figure 4.6 Conducted EMI noise spectrum with hybrid filter (Simulation)

Table 4.2 Comparison between the experimental and simulation results

Harmonic Frequency	Hybrid Filter Attenuation	Hybrid Filter Attenuation

(MHz)	(dBuV) (Simulation)	(dBuV) (Experimental)
0.7	34	31
1.4	42	36.5
2.1	50.1	29.8
2.8	46.1	35.3
3.5	53	37.4

4.5 Conclusions

This chapter aims to provide the complimentary information that can not be included in the journal paper due to text redundancy. Details on the test setup and measurements of the proposed EMI filter circuit have been presented. Moreover, simulation and experimental results have been compared and their similarities have been summarized.

Chapter 5

Conclusions and Recommendations

This master thesis has explored some filtering techniques of the conducted EMI noise mitigation, including passive filter, active filter, and the combined passive/active (hybrid) filter. For each type of EMI filter, the circuit configurations, design considerations, performance evaluation and limitations have been presented.

Passive filters have been the quick fix solution for most of the power system engineers due to its simplicity and low cost, especially when they are confronted with the EMI noise generated by DC/DC converters. However, because of the constraints of the size, weight, temperature and reliability, the performance of the passive EMI filter cannot meet very stringent EMC requirements at low frequencies.

Active filters have been an alternative solution for EMI noise mitigation at low frequencies (around switching frequency). However, it has poor performance at very high frequencies due to the inherent phase error generated by the active components.

As demonstrated in this master thesis, active EMI filters are best used when combined with passive filters, namely hybrid EMI filters at the input side of the DC/DC converter, to reduce low frequency harmonic noise which can not be achieved with a sole passive filter, and to reduce the size of the passive filter with minimum cost and power losses. A

new type of hybrid EMI filter has been proposed to meet the requirements of the full EMC spectrum according to the CISPR22 standard. Its configuration is developed based on the following design preferences:

1. The active EMI filter is placed at the input side of the DC/DC converter to minimize the size of the passive EMI filter components.
2. placing the active EMI filter at the input side will provide the flexibility of the filter to be used most of the DC/DC converters regardless of their topologies, since it does not interfere with the feedback loop of the converter (Peng et al., 2005), should this latter be placed at the output of the converter.
3. A simple RC branch circuit is used to detect the noise voltage signature, instead of using magnetic transformer that have to carry full primary DC current of the converter and produce thermal loss.
4. The active EMI filter circuit is referenced to ground instead of the power return. This type of circuit connection aims to attenuate CM noise which is the dominant (80%) noise in DC/DC converter circuits (Junichi et al., 2002).

Finally, we have explained the differences and the similarities that exist between the simulation and the experimental measurements. It is found that the overall simulated EMI noise spectrum is closely comparable to that found in the experimental prototype, while the differences are due to the limitation of the component models.

Regarding the future work, it is recommended that the active EMI filter circuit could be replaced by a digital EMI filter that accomplishes noise reduction in both the low and the high frequency regions. This will remove the requirements of the passive EMI filter being perpetual in the DC/DC converter circuit. With today's high speed Digital Signal Processors (DSP), it is possible to implement and develop an algorithm to convert the EMI analog signal into digital signal (A/D converter), process the data signal and convert it back to its original analog signal through an D/A converter and inject it back to the DC bus to cancel out the incident noise. This will further improve the circuit geometry in vocabulary of weight, size, as well as costs and time to market.

REFERENCES

ANSI C63.022, (1996). American National Standards for limits and methods of measurements of radio disturbance characteristics of information technology equipment, pp. 12-30.

CHOI, B., BO H. C., (1995) "Intermediate Line Filter Design to Meet both Impedance Compatibility and EMI Specifications" IEEE Transactions on Power Electronics, Vol. 10, No. 5, pp. 583-588

DJILALI, H., SAWAN, M. (October 2006). Conducted noise mitigation in DC/DC converters using active filtering method. Submitted to IEEE Transactions on Industrial Electronics, currently under review.

EN55022, CISPR22. (1995) Information Technology Equipment (ITE) – Radio disturbance characteristics – Limits and methods of measurement, pp. 10 – 62.

EN55011, (1999) Limits and methods of measurement of radio disturbance characteristics of industrial, scientific and medical (ISM) radio frequency equipment, pp. 12 – 87.

FARKAS, T., and SCHLECHT, M.F., (1994) "Viability of active EMI filters for utility applications" IEEE Transactions on Power Electronics, Vol. 9, No. 3, pp. 328-337.

FRANC, M., DEJAN K., (2006) "Reduced Conductive EMI in Switched-Mode DC-DC Power Converters without EMI Filters: PWM versus Randomized PWM" IEEE Transactions on Power Electronics, Vol. 21, No.6, pp. 1776-1782.

GUO T., DAN Y. C., FRED C. LEE, (1996) "Separation of the Common-mode and Differential-mode conducted EMI noise" IEEE Transactions on Power Electronics, Vol.11, No.3, pp. 480 -488.

JUNICHI, M., MASAYUKI, M., (2002) "Measurement of the Source Impedance of Conducted Emission Using Mode Separable LISN" Electrical Engineering in Japan, Vol. 139, No, 2, pp. 1376-1381.

LASZLO T., (1995) "Electromagnetic Compatibility in Power Electronics" IEEE Press, New York, 1995.

LAWHITE, L.E., and SCHLECHT, M.F, (1988) "Design of active ripple filters for power circuits operating in the 1-10MHz range" IEEE Transactions on Power Electronics, Vol 3, No 3, pp. 310 -317.

LEE, D.Y. CHO, B.H. (1996) "Design of an input filter for power factor correction (PFC) AC to DC converters employing an active ripple cancellation" Energy Conversion Engineering Conference. Proceedings of the 31st Intersociety, Vol.1, pp. 582 – 586.

MARTIN F.L., ARTHUR F.W., (1996) "Input filter Design for multiple-module DC power systems" IEEE Transactions on Power Electronics, Vol.11, No.3, pp. 472 – 488.

MIDDLEBROOK, R. D., (1976) Input Filter Considerations in Design and Application of Switching Regulators, IEEE Industry Applications Society, Annual Meeting, 1976 Record, 366—382 (IEEE Publication 76CH1122-1-IA).

MINGJUAN Z., DAVID J. P., (2005) "Design and Evaluation of feed-forward Active Ripple Filters" IEEE Transactions on Power Electronics, Vol. 20, No. 2, pp. 276 – 285.

PENG, Li, Brad, L., (2005) " Accurate Loop Gain Prediction for DC-DC converter Due to the Impact of Source/Input Filter" IEEE Transactions on Power Electronics, Vol. 20, No. 4, pp. 754-761.

PICOR CORPORATION (2006). The QPI family of active EMI filter, www.picorpower.com.

SCHAFFNER (2006). FN family of PCB mount passive EMI filter, www.schaffnerusa.com.

TEXAS SPECTRUM ELECTRONICS (2006). The CF filter family, Custom design passive filters for space applications, www.texasspectrum.com.

YUK, K.W., YIM-SHU, L. and DAVID, K.C, (2000) "Synthesis of a wide bandwidth current sensor using a current transformer for active power filter applications" IEEE-PESC, Vol.1, pp. 270 – 273.

APPENDIX A

MathCAD Design Files

This appendix contains the MathCAD design files used in this project. It is a tool to calculate the design parameters of the DC/DC converter under different load conditions. It also, contains the plots of the insertion loss vs. frequency and the plot of the noise attenuation transfer function of the hybrid active and passive EMI filter with different input inductor values.

A.1 30 W DC/DC FORWARD CONVERTER DESIGN

Units Definition

$Ohm := 1$

$mOhm := 10^{-3}$

$Ohm := 1 \qquad mOhm := 10^{-3}$

$W := 1 \qquad kHz := 100$

Hysteresis coefficient

$V := 1 \qquad A := 1$

$T := 1 \qquad \mu H := 10^{-6}$

$mJ := 10^{-3}$

Eddy Current Coefficient

$Kh := 4 \cdot 10^{-5}$

$Ke := 4 \cdot 10^{-10}$

$\mu o := 4 \cdot \pi \cdot 10^{-7}$

$mm := 10^{-3} \qquad cm := 0.01$

$Kf := 3$

$Kff := 0.15$

$scm := 1$

A.1.1. Input Data

smm := 0.01

Maximum Output Power

$P_{omax} = 30W$

Minimum Output Power

$P_{omin} = 0.15 \cdot P_{omax}$

Pomin = 4.5W

Minimum Line Voltage

$V_{inmin} = 17$ Volts

Maximum Line Voltage

Vinmax := 60 · V

Efficiency Assumed

η := 0.8

Switching Frequency

$F_s = 700$ KHz

Maximum Duty Cycle

Dmax := 0.65

Output 1 Nominal Voltage

U1 := 5 · V

Output 1 Maximum Current

$I_{1max} = 4$ Amps

$I_{1min} = 0.15 \cdot I_{1max}$

IRF640S MOSFET

FET R_{dson} @ 25 deg C

$tr := 44 \cdot 10^{-9}$ Rdson := 0.044 $tf := 43 \cdot 10^{-9}$ $Coss := 250 \cdot 10^{-12}$

A.1.2. General Considerations

Output parameters Transferred to Output 1

Output 1 Nominal Voltage

$U_0 = 5$ Volts

Output 1 Maximum Current

I0max:= 4·A

Output 1 Minimum Current

I0min := 0.15 · I0max

I0min = 0.6 A

Rectifier Diodes Voltage Drop

Vd := 0.7 · V

Current Sense Resistor

Rs := 0 · Ohm

Max FET Current at Low Line

$$Ipkll := \frac{Pomax}{Vinmin \eta \cdot Dmax}$$

Ipkll = 3.394A

Turns Ratio Required

- Secondary to Primary

$$N21 := \frac{U0 + Vd}{Vinmin - Ipkll \cdot Rdson - 0.5} \cdot \frac{1}{Dmax}$$

N21 = 0.536

- Primary to Secondary

$N12 := N21^{-1}$ N12 = 1.865

!!! Turns Ratio Adjustment Point !!!

N12 := 0.65 $N21 := N12^{-1}$ N21 = 1.538

Duty Cycle @ High Line

$$Dmin := \frac{(U0 + Vd) \cdot N12}{Vinmax - 0.5 - \frac{I0max \cdot Rdson}{N12}}$$ Dmin = 0.063

Max FET Current at High Line

$$Ipkhl := \frac{Pomax}{Vinmax \eta \cdot Dmin}$$ Ipkhl = 9.991A

A.1.3. TRANSFORMER DESIGN

Topology Coefficient (Idc/Irms)

Kt := 0.71

Winding Factor (Window Area Used/ Full Window Area)

Ku := 0.4

Part of Window Area Occupied by Primary

Kp := 0.5

Area Product required for 3F3 material from Philips

$f = 700 \quad kHz$

$$AP(f) := \left(\frac{Dmax \cdot Pomax \cdot 10^4}{88 \cdot \eta \cdot Kt \cdot Ku \cdot Kp \cdot f} \right)^{1.873} \cdot \left(Kh \cdot f + Ke \cdot f^2 \right)^{0.624}$$

$AP(f) = 0.036 \ cm\text{^}4$

Core EFD 20 has the following Parameters

$Ae20 := 0.31 \qquad Aw20 := 0.29 \qquad Vc20 := 1.46 \qquad \mu c := 1450$

$AP := Ae20 \cdot Aw20 \qquad lmag := 4.7 \qquad Al := 1.2 \cdot \mu H \qquad MTL := 3.59 \cdot cm$

$AP = 0.09 \ cm\text{^}4$

Current Density for 15 deg C temperature Rise due to the Copper Losses

$J15 := 297 \cdot AP^{-0.24} A/cm\text{^}2 \qquad J15 = 529.486$

Adjusted Value of Current Density

$J15 := 1 \cdot J15 \qquad J15 = 529.486$

Maximum B_m that provides 15 deg C temperature Rise due to the Core Losses

$Kf := 3 \qquad Kff := 0.15$

$Bm(f) = 0.045T$

$$Bm(f) := \frac{0.405 \cdot (Ae20 \cdot Aw20)^{-\frac{0.31}{Kf}}}{\left(\frac{Kh \cdot f + Ke \cdot f^2}{Kff} \right)^{\frac{1}{Kf}}}$$

Core Losses

$$Pcloss := Vc20 \left[\frac{Bm(f)^{Kf}}{Kff} \cdot \left(Kh \cdot f + Ke \cdot f^2 \right) \right]$$

$Pcloss = 0.205W$

Assuming Copper Losses Equal to the Core Losses

$Pcoploss := Pcloss$

Estimated Transformer Temperature Rise

$\Delta T := (Pcloss + Pcoploss) \cdot 23 \cdot AP^{-0.37}$ $\Delta T = 22.957$

$Vinmin := Vinmin - \frac{Rdson \cdot Ipkhl}{N12} - 0.5$ $Vinmin = 15.824\ V$

Minimum Number of Primary Turns

$Np := \frac{Vinmin\,Dmax}{(Bm(f)) \cdot Ae20 \cdot f} \cdot 10^4$ $Np = 10.429$

Rounded Number of Turns

Primary Inductance

$Nwp := 12$ $Lp := Al \cdot Nwp^2$ $Lp = 172.8\mu H$

Number of Turns at the secondary

$Nw10 := Nwp \cdot N21$ $Nw10 = 18.462$

Secondary Inductance

$Ls := Al \cdot Nw10^2$ $Ls = 408.994\mu H$

Magnetization Current

Check Point

$Imag := \frac{VinmaxDmin}{f \cdot Lp}$ $\Delta Btxf := \frac{VinmaxDmin}{Nwp \cdot Ae20 \cdot f} \cdot 10^4$ $Imag = 0.031A$

$\Delta Btxf = 0.014T$ $Bmtxf := \frac{\Delta Btxf}{2}$

$Bmtxf = 7.207 \times 10^{-3}\,T$

TXF Core Losses

$$Ptxfcloss := Vc20\left[\frac{Bmtxf^{Kf}}{Kff}\cdot\left(Kh\cdot f + Ke\cdot f^{2}\right)\right]$$

$Ptxfcloss = 8.16 \times 10^{-4}\,W$

Primary RMS Current at Low Line

$$Iprmsll := \frac{Pomax}{\eta \cdot Vinmin}$$

$Iprmsll = 2.37A$

FET Conduction Losses

Sense Resistor Losses

$Pfetcdll := Iprmsll^{2}\cdot Rdson\cdot 1.5$

$Rs = 0\,Ohm$

$Psll := Iprmsll^{2}\cdot Rs$

$Psll = 0\,W$

$Pfetcdll = 0.371W$

$$Pswoffll := (Ipkll + Imag)\cdot Vinmin\,tf\cdot\frac{f}{8}$$

$$Pswonll := \frac{Coss\cdot Vinmin^{2}}{2}\cdot 1$$

$Pswoffll = 0.204W$

$Pswonll = 0.022W$

$Pfetll := Pfetcdll + Pswoffll + Pswonll$

$Pfetll = 0.596W$

Primary RMS Current at High Line

$$Iprmshl := \frac{Pomax}{\eta \cdot Vinmax}$$

$Iprmshl = 0.625A$

FET Conduction Losses

Sense Resistor Losses

$Pfetcdhl := Iprmshl^2 \cdot Rdson \cdot 1.5$ $Pshl := Iprmshl^2 \cdot Rs$ $Pfetcdhl = 0.026W$

Switching Losses

$Pshl = 0\,W$ $Pswoffhl := (Ipkhl + Imag) \cdot Vinmaxtf \cdot \frac{f}{8}$

$Pswonhl := \frac{Coss \cdot Vinmax^2}{8} \cdot f$

$Pswoffhl = 2.263W$ $Pswonhl = 0.079W$ $Pfethl := Pfetcdhl + Pswoffhl + Pswonhl$

$Pfethl = 2.367W$

TRANSFORMER COPPER LOSSES

Primary current varies with input line drastically. Calculations to the primary winding were done to some intermediate current which is calculated from the following expression.

$$Ipw := \sqrt{\frac{Iprmsll^2 + Iprmshl^2}{2}} \qquad Ipw = 1.733$$

Required wire cross section area

$Swp := \frac{Ipw}{J15}$ $Swp = 3.273 \times 10^{-3}$

$Dwp := 2 \cdot \sqrt{\frac{Swp}{\pi}}$ $Dwp = 0.065$

Copper Specific Resistance

$\rho(T) := 1.724[1 + 0.0042(T - 20)] \cdot 10^{-8}$ Receptivity in W/m

Resistance of the Primary Winding

$\rho(T) = 1.586\times 10^{-8}$ $\quad$ $Rwpdc := \frac{Nwp \cdot MTL \cdot \rho(100)}{Swp} \cdot 10^{4}$ $\quad$ $Rwpdc = 0.03$

Skin Depth

$$\delta := \frac{1}{2\cdot\pi}\cdot\sqrt{\frac{\rho(T)}{f\cdot 10^{-7}}}$$

$\delta = 0.076mm$

$$Q := \frac{Dwp\cdot 10^{-2}}{\delta}\cdot 0.866$$

$Q = 7.379$

Resistance factor due to Skin Effect

$Q := 0.5, 0.6 .. 2.5$ $\quad$ $F(Q) := Q$

$$Frskin(Q) := Q\cdot\frac{e^{2\cdot Q} - e^{-2\cdot Q} + 2\cdot\sin(2\cdot Q)}{e^{2\cdot Q} + e^{-2\cdot Q} - 2\cdot\cos(2\cdot Q)}$$

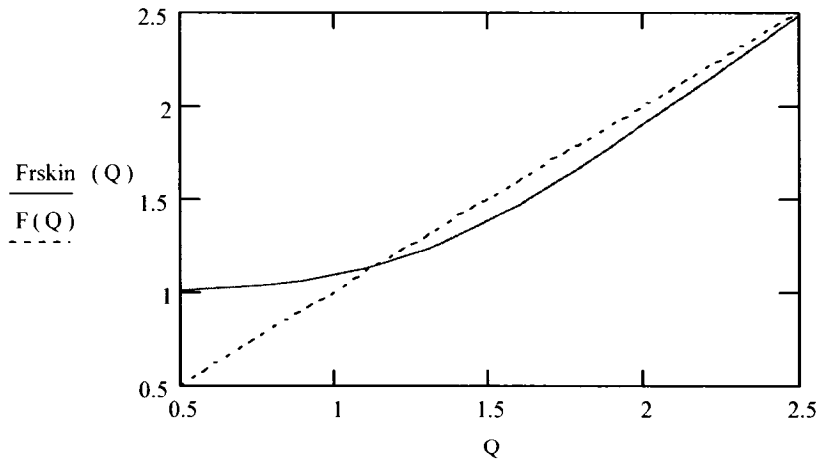

Figure A.1 Variation of the resistance factor due to skin effect

$$Q := \frac{Dwp\cdot 10^{-2}}{\delta}\cdot 0.866$$

$Q = 7.379$ $\quad$ $Frskin(Q) = 7.379$

Primary Resistance to Alternative Current

$Rpwac := Frskin(Q) \cdot Rwpdc$ $\quad$ $Rpwac = 0.224$ $\quad$ $Ppll := Iprmsll^2 \cdot Rpwac$

$Pphl := Iprmshl^2 \cdot Rpwac$ $\quad$ $Ppll = 1.256$ $\quad$ $Pphl = 0.087$

Single wire can not be used because of high skin effect factor. Q should be reduced to at least Q<1.5, by reducing wire diameter.

Maximum Wire Gage that can be used

$Dwps := 1.4 \cdot \delta \cdot 100$ $\quad$ $Dwps = 0.011$ $\quad$ $AWG := -20 \cdot \log\left(Dwps \cdot \frac{\pi}{2.54}\right)$

$AWG = 37.641$

Point of Adjustment

$AWG := 34$

Number of Strands Required for Primary

$$Dwps := \frac{2.54}{\pi} \cdot 10^{-\frac{AWG}{20}}$$

$$Swps := \frac{\pi \cdot Dwps^2}{4}$$

$$Nps := \frac{4 \cdot Swp}{\pi \cdot Dwps^2}$$

$Nps = 16.014$

Point of Adjustment

$Nps := 22$

DC Resistance of the Primary Winding

$$Rwpdc := \frac{Nwp \cdot MTL \cdot \rho(100)}{Nps \cdot Swps} \cdot 10^4$$

$Rwpdc = 0.022$

AC Resistance of the Primary Winding

$$Q := \frac{Dwps \cdot 10^{-2}}{\delta} \cdot 0.866$$

$Q = 1.844$

$Rpwac := Frskin(Q) \cdot Rwpdc$ $\quad Frskin(Q) = 1.72$ $\quad Rpwac = 0.038$

Primary Winding Copper Losses

Low Line

$Ppll := Iprmsll^2 \cdot Rpwac$

$Ppll = 0.213\ W$

High Line

$Pphl := Iprmshl^2 \cdot Rpwac$

$Pphl = 0.015\ W$

Copper Losses in Transformer Secondary

Low Line

$$I1pk := I1max + \frac{I1min}{2}$$

$$I1l := I1max - \frac{I1min}{2}$$

$$Irms10ll := \sqrt{Dmax\left[\frac{I1pk^2 + I1pk \cdot I1l + I1l^2}{3} - \frac{Dmax}{4}\cdot(I1pk + I1l)^2\right]}$$

Irms10ll= 1.913A

High Line

$$I1pk := I1max + \frac{I1min}{2} \qquad I1l := I1max - \frac{I1min}{2}$$

$$Irms10hl := \sqrt{Dmin\left[\frac{I1pk^2 + I1pk \cdot I1l + I1l^2}{3} - \frac{Dmin}{4}\cdot(I1pk + I1l)^2\right]}$$

Irms10hl = 0.97A

Total TXF Losses

Low Line

High Line

Ptxfll:= Pw10ll+ Ppll + Ptxfcloss Ptxfhl := Pw10hl + Pphl + Ptxfcloss Ptxfll= 0.508W

Ptxfhl = 0.091W

OUTPUT CHOKE DESIGN

Minimum Combined Output Current

I0min = 0.6 A

To secure continuous current in output choke (I0min>ΔI0/2), assume

$\Delta I0 := 2 \cdot I0min$ $\Delta I0 = 1.2$

I0min = 0.6 A

Peak Output Choke Current

$$I0pk := I0max + \frac{\Delta I0}{2}$$

I0pk = 4.6 A

Minimum Inductance Required

$$Lmin := \frac{(U0 + Vd)\cdot(1 - Dmin)}{2\cdot I0min\cdot f}$$

Lmin = 6.361μH

Adjusted Value

Lmin := 1 · Lmin Lmin = 6.361μH

Energy Stored in the Choke

$$Wck := \frac{Lmin\, I0pk^2}{2}$$

Wck = 0.067mJ Bmax := 0.25·T Kw := 0.5

$$APch := \frac{2\cdot Wck\cdot 10^4}{Bmax\, Kw\cdot J}$$

APch = 0.02

The same EFD 20 core from Philips could be used for the Coupled Choke

Minimum Number of Turns

$$Nch := \frac{Lmin\cdot I0pk}{Bmax\cdot Ae20}\cdot 10^4$$

Nch = 3.776

The Gap

$$Gap := \frac{\mu o\cdot Nch^2\cdot Ae20}{Lmin}\cdot 10^{-4}$$

Gap = 0.087 mm

$$Alck := \frac{Lmin}{Nch^2}$$

$Alck = 0.446\mu H$

Point of Adjustment

$Alck := 0.1 \cdot \mu H$

Output 1 Inductance

$$Lck10 := \frac{2 \cdot Wck}{I1max^2}$$

$Lck10 = 8.413\mu H$

$$Nck10 := \sqrt{\frac{Lck10}{Alck}}$$

$Nck10 = 9.172$

Point of Adjustment

Number of turns should be rounded to the closest integer

$Nck10 := 9$

Choke Windings Inductances Recalculated IAW New Number of Turns

$Lck10 := Alck \cdot Nck10^2$

$Lck10 = 8.1\mu H$

$$\Delta Bmck := \frac{\left(Vinmax\frac{Nw10}{Nwp} - U1 - Vd\right) \cdot Dmin}{Nck10 \cdot Ae20 \cdot f} \cdot 10^4$$

$\Delta Bmck = 0.028T$

Relative Core Permeability with a Gap

$$\mu c := \frac{Lck10 \cdot lmag \cdot 100}{\mu o \cdot Nck10^2 \cdot Ae20}$$

$\mu c = 120.65$

DC Flux Density

$$Bdc := \frac{0.4 \cdot \pi \cdot \mu c \cdot Nw10 \left(I1max + \frac{I1min}{2} \right)}{lmag}$$

$Bdc = 2.561 \times 10^3$

B_{max} should be less than

$$Bmax := Bdc + \frac{\Delta Bmck}{2}$$

$Bmax = 2.561 \times 10^3 \, T$

$$Bac := \frac{\Delta Bmck}{2}$$

$Bmax = 2.561 \times 10^3 \, T$

Choke Core Losses

$Bac = 0.014T$

$$Pckcore := Vc20 \left[\frac{Bac^{Kf}}{Kff} \cdot \left(Kh \cdot f + Ke \cdot f^2 \right) \right]$$

$Pckcore = 5.818 \times 10^{-3} \, W$

COPPER LOSSES IN THE CHOKE WINDINGS

$$Ick10rms := \frac{2 \cdot I1max}{\sqrt{3}}$$

$Ick10rms = 4.619A$ $Ick10rms = 4.619A$ $Sck10 := \frac{Ick10rms}{J15}$

$Dck10 := 2 \cdot \sqrt{\frac{Sck10}{\pi}}$

$AWGck10 := -20 \cdot \log\left(Dck10 \frac{\pi}{2.54}\right)$

$AWGck10 = 17.698$

Point of Adjustment

Wire Gauge Chosen

$AWGck10 := 20$

Number of Strands

$Dsck10 := \frac{2.54}{\pi} \cdot 10^{-\frac{AWGck10}{20}}$

$Ssck10 := \frac{\pi \cdot Dsck10^2}{4}$

$Nsck10 := \frac{4 \cdot Sck10}{\pi \cdot Dsck10^2}$

Number of Strands Recommended $Nsck10 = 1.699$

Point of Adjustment $Nsck10 := 2$

DC Resistance and Losses of the Choke Windings

$Rck10dc := \frac{Nck10 \cdot MTL \cdot \rho(100)}{Nsck10 \cdot Ssck10} \cdot 10^4$

$Rck10dc = 7.248mOhm$ $Pck10 := Ick10rms^2 \cdot Rck10dc$ $Pck10 = 0.155\ W$

$Pcktot := Pck10 + Pckcore$ $Pcktot = 0.16W$

EFFICIENCY

Pcntr := 0.36 W Prec := 11maxVc Prec = 2.8 W Pother := 0.5 W

Low Line

$$\eta ll := \frac{Pomax}{Pomax + Pfetll + Ptxfll + Pcktot + Pcntr + Prec + Pother + Psll}$$

$\eta ll = 85.899\%$

High Line

$$\eta hl := \frac{Pomax}{Pomax + Pfethl + Ptxfhl + Pcktot + Pcntr + Prec + Pother + Pshl}$$

$\eta hl = 82.693\%$

END of File

A.2. MISMATCHED IMPEDANCE CALCULATIONS

$w(f) := 2 \cdot \pi \cdot 1$ $L1 := 10 \cdot 10^{-6}$ (Henries) $C1 := 1 \cdot 10^{-6}$ (Farads)

$$f0 := \frac{1}{2\pi\sqrt{L1 \cdot C1}}$$ The resonance frequency of the LC circuit

$f0 = 5.033 \times 10^{4}$

$w0(f0) := 2 \cdot \pi \cdot f0$ Angular Frequency $f := 1000, 2000 .. 10 \cdot 10^{6}$

1. Insertion Loss vs. Frequency under Resistive load impedance

$$IL(f, R1) := \sqrt{\left(1 - \frac{w(f)^2}{w0(f0)^2}\right)^2 + \frac{(w(f) \cdot L1)^2}{R1^2}}$$

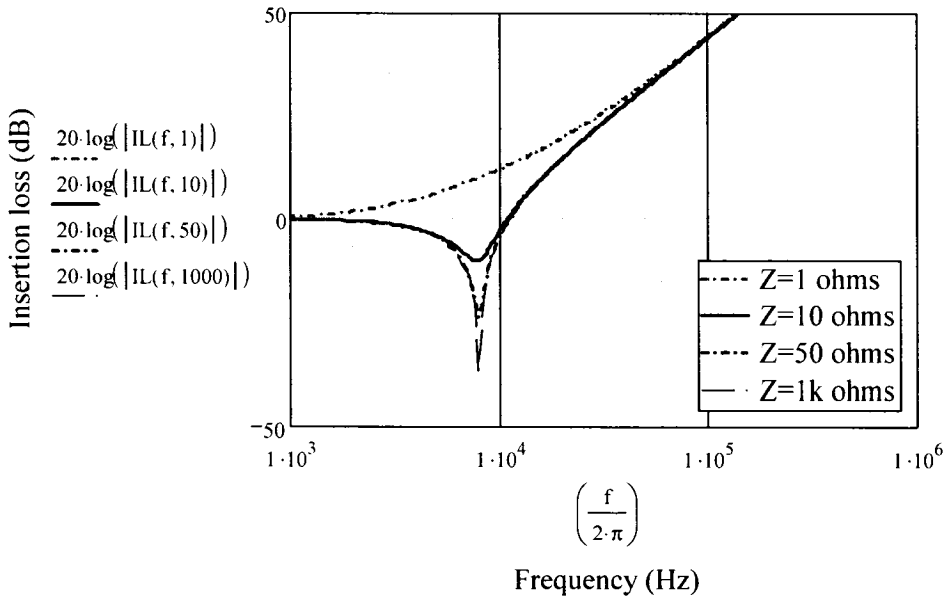

Figure A.2 Insertion Loss vs. Frequency under Resistive load impedance

2. Insertion loss vs. frequency under Inductive impedance load

$$L2 := 1 \cdot 10^{-6}$$

$$w1(f) := \sqrt{w0(f0)^2 \left(1 + \frac{L1}{L2}\right)}$$

$$IL1(f, R1) := \left(1 + \frac{L2}{L1}\right) \cdot \sqrt{\left(1 - \frac{w(f)^2}{w1(f)^2}\right)^2 + \frac{(w(f) \cdot L1)^2}{R1^2} \cdot \frac{1}{1 + \frac{L1}{L2}}}$$

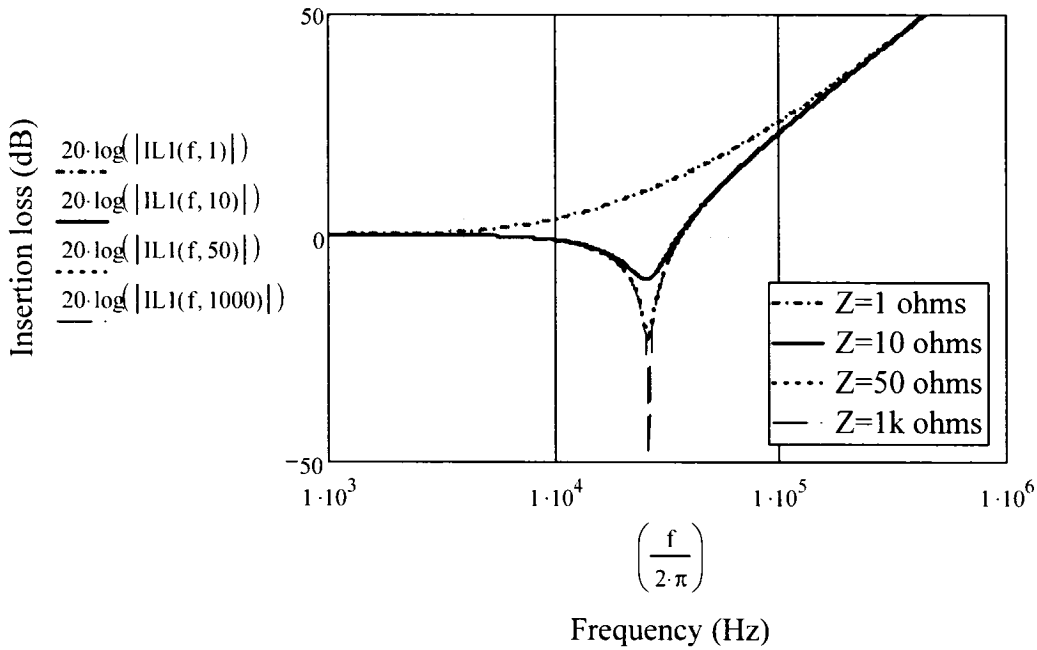

Figure A.3 Insertion loss vs. frequency under Inductive impedance load

3. Insertion loss vs. frequency under capacitive impedance load

$$C2 := 10 \cdot 10^{-6}$$

$$w3(f) := \sqrt{\frac{w0(f0)^2}{1 + \frac{C2}{C1}}}$$

$$IL2(f, R1) := \sqrt{\left(1 - \frac{w(f)^2}{w3(f)^2}\right)^2 + \frac{(w(f) \cdot L1)^2}{R1^2}}$$

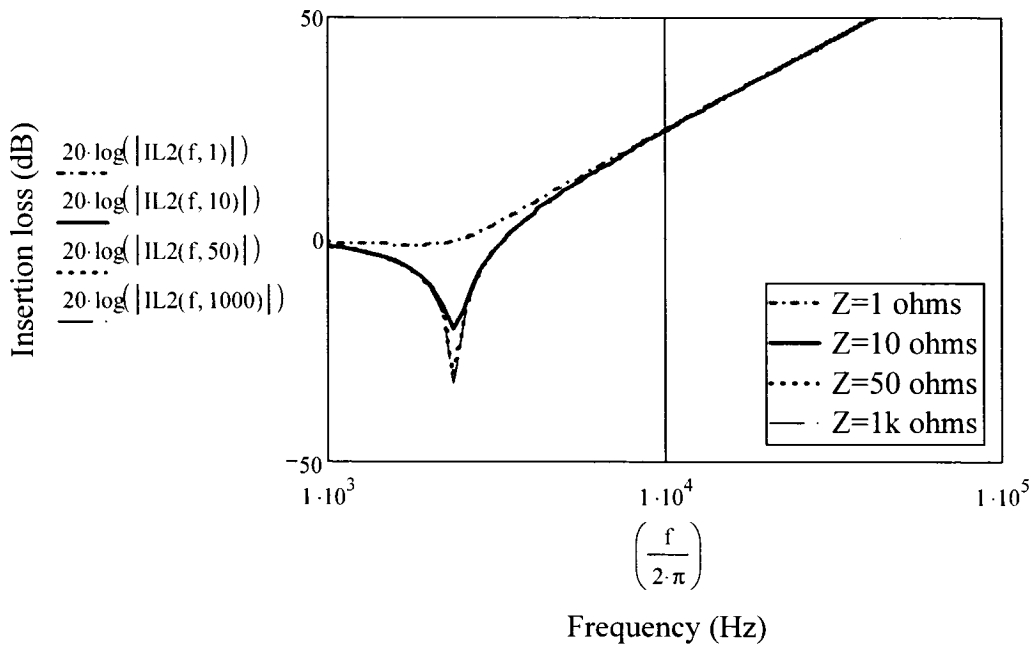

Figure A.4 Insertion loss vs. frequency under capacitive impedance load

A.3 NOISE ATTENUATION TRANSFER FUNCTION

$Zin := 0.1$ $\quad Lin := 2 \cdot 10^{-6}$ $\quad j := \sqrt{-1}$ $\quad w(f) := 2 \cdot \pi \cdot f$

$j^2 = -1$

$f := 1000, 1500 .. 10 \cdot 10^6$

$k := 30$

$$Av(f) := \frac{2 \cdot 10^6 \cdot k}{1 + j \cdot \frac{w(f)}{15}}$$

$Cin := 20 \cdot 10^{-6}$

$$k(Lin) := \frac{100}{w\left(700 \cdot 10^3\right) \cdot Lin}$$

$$Av(f, Lin) := \frac{20 \cdot 10^{6} \cdot k(Lin)}{1 + j \cdot \frac{w(f)}{50}}$$

$$Zin(f) := 0.1$$

$$k\left(2 \cdot 10^{-6}\right) = 11.368$$

$$Cin := 20 \cdot 10^{-6}$$

$$Av1(f, Lin) := \frac{6 \cdot 10^{6}}{1 + j \cdot \frac{w(f)}{100}}$$

$$N := \frac{50}{w\left(700 \cdot 10^{3}\right) \cdot 1 \cdot 10^{-6}}$$

$$L := 50 \cdot 10^{-6} \qquad N = 11.368 \qquad R := 50$$

$$Zin(f) := \frac{R \cdot j \cdot w(f) \cdot L}{R + j \cdot w(f) \cdot L}$$

$$\left|Zin\left(1 \cdot 10^{6}\right)\right| = 49.379$$

$$Av(f, Lin) := \frac{-Av1(f, Lin)}{2 + Av1(f, Lin)}$$

$$M1(f, Lin) := \frac{1}{1 + j \cdot w(f) \cdot Cin \cdot (Zin(f) + j \cdot w(f) \cdot Lin)}$$

$$k\left(2 \cdot 10^{-6}\right) = 11.368$$

$$Cs := 15 \cdot 10^{-6} \qquad Rs := 200 \qquad f\_s := \frac{1}{Rs \cdot Cs}$$

$$f\_s = 333.333$$

$$E(f, Lin) := Rs \cdot (1 + Av(f, Lin) \cdot k(Lin)) + \frac{1}{j \cdot w(f) \cdot Cin}$$

$$F(f, Lin) := \frac{-1}{j \cdot w(f) \cdot Cs} - Av(f, Lin) \cdot k(Lin) \cdot Rs \cdot \left[\frac{Rs \cdot (1 + Av(f, Lin) \cdot k(Lin))}{E(f, Lin)} - 1 \right]$$

$$M3(f, Lin) := Rs \cdot \frac{1}{j \cdot w(f) \cdot Cin \cdot E(f, Lin)} + \frac{1}{j \cdot w(f) \cdot Cs} \cdot \frac{1}{j \cdot w(f) \cdot Cin \cdot E(f, Lin)} \cdot \frac{1}{(j \cdot w(f) \cdot Lin) + \frac{1}{j \cdot w(f) \cdot Cs}}$$

$$M4(f, Lin) := Zin(f) + Rs \cdot \left[1 - \frac{Rs \cdot (1 + Av(f, Lin) \cdot k(Lin))}{E(f, Lin)} \right] + \frac{1}{j \cdot w(f) \cdot Cs} \cdot \left[1 + \frac{F(f, Lin)}{(j \cdot w(f) \cdot Lin) + \frac{1}{j \cdot w(f) \cdot Cs}} \right]$$

$$M2(f, Lin) := \frac{M3(f, Lin)}{M4(f, Lin)}$$

$$NA(f, Lin) := \frac{M2(f, Lin)}{M1(f, Lin)}$$

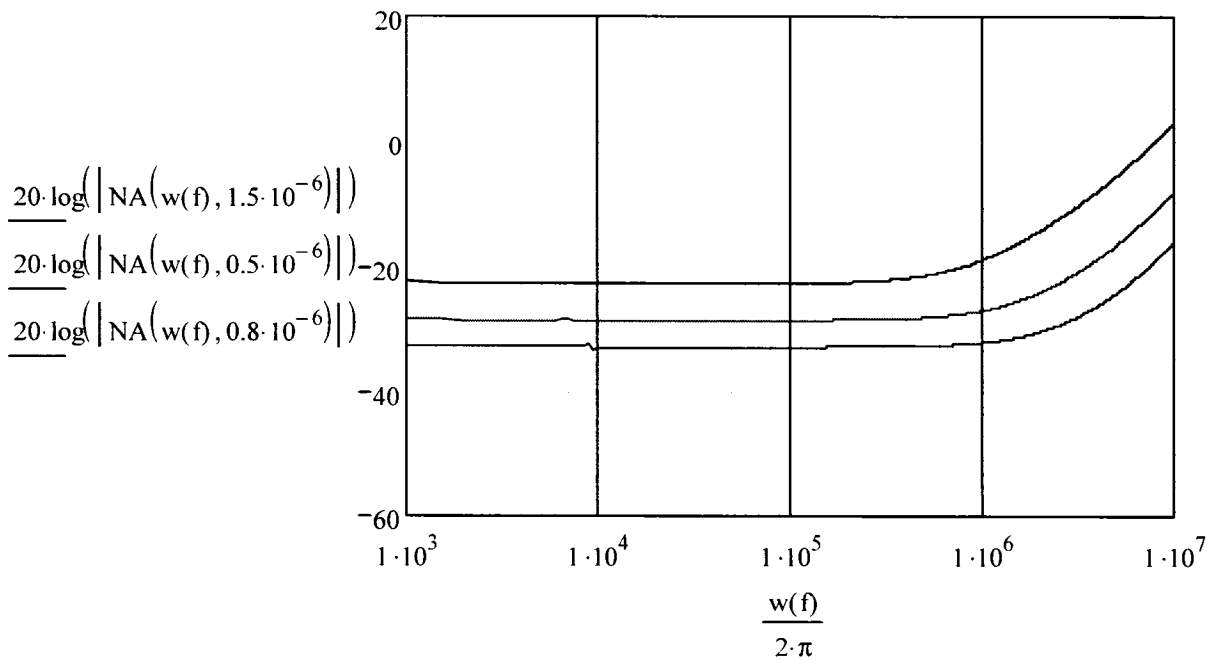

Figure A.5 Plot of the Noise Attenuation Transfer Function versus Frequency

A.4. NOISE ATTENUATION FOR VOLTAGE AND CURRENT NOISE INJECTION ACTIVE CIRCUIT

$$j := \sqrt{-1} \qquad f := 1\cdot 10^3, 2\cdot 10^3 .. 30\cdot 10^6 \qquad w(f) := 2\cdot\pi\cdot f$$

$$C := 1\cdot 10^{-6} \qquad Zin(w) := \frac{100\, j\cdot w\cdot 100\cdot 10^{-6}}{100 + j\cdot w\cdot 100\cdot 10^{-6}} \qquad A(w,n,m) := \frac{m\cdot 10^6}{\left(1 + \frac{j\cdot w}{n\cdot 2\cdot\pi}\right)}$$

$$K(w,n,m) := 1 - \frac{1}{1 + A(w,n,m)}$$

$$NA_V(w,n,m) := \frac{1 - K(w,n,m)}{1 - K(w,n,m) + j\cdot w\cdot Zin(w)\cdot C}\cdot(1 + j\cdot w\cdot Zin(w)\cdot C)$$

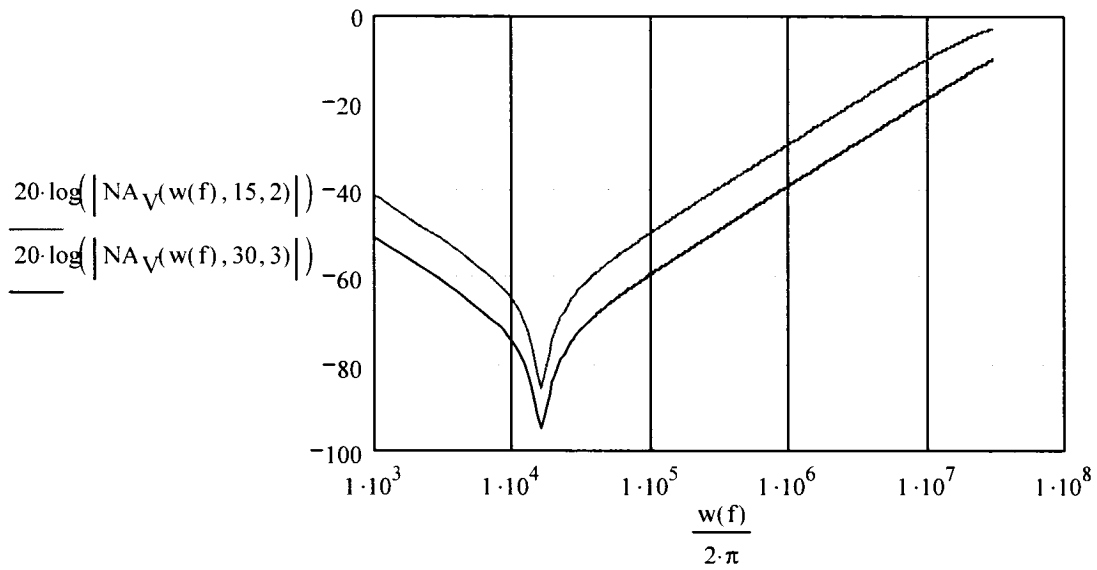

Figure A.6 Noise Attenuation for voltage noise injection active circuit

$$G(w, n, m) := 1 - \frac{1}{1 + A(w, n, m)}$$

$$NA_I(w, n, m) := 1 - G(w, n, m)$$

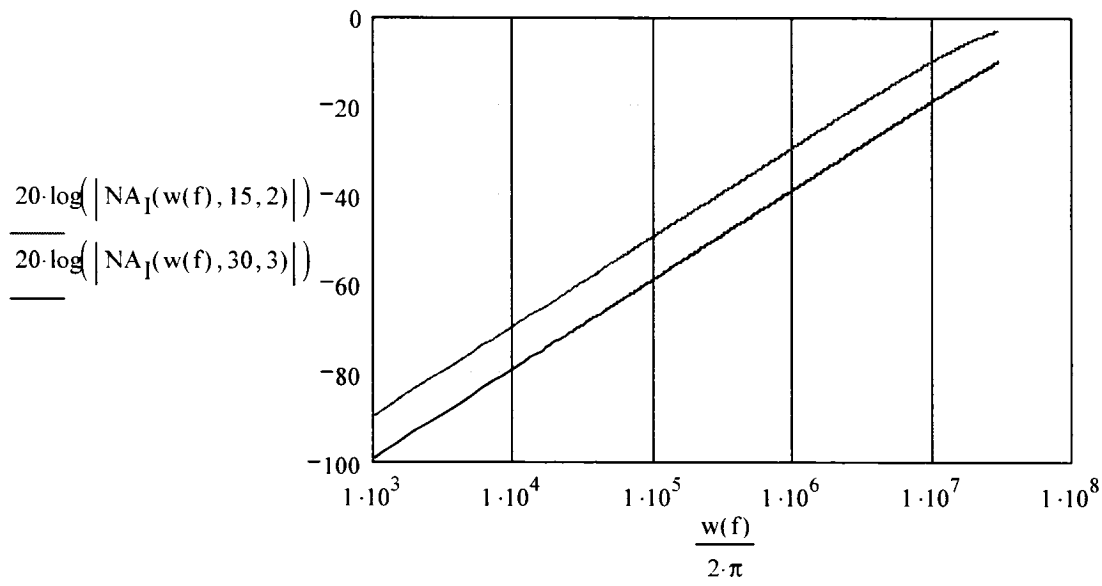

Figure A.7 Noise Attenuation for current noise injection active circuit

APPENDIX B

Schematic and PCB Layout Files

This appendix contains relevant schematic and PCB design files using PSPICE software. The components list is also included in this appendix.

B.1. Schematic Diagram

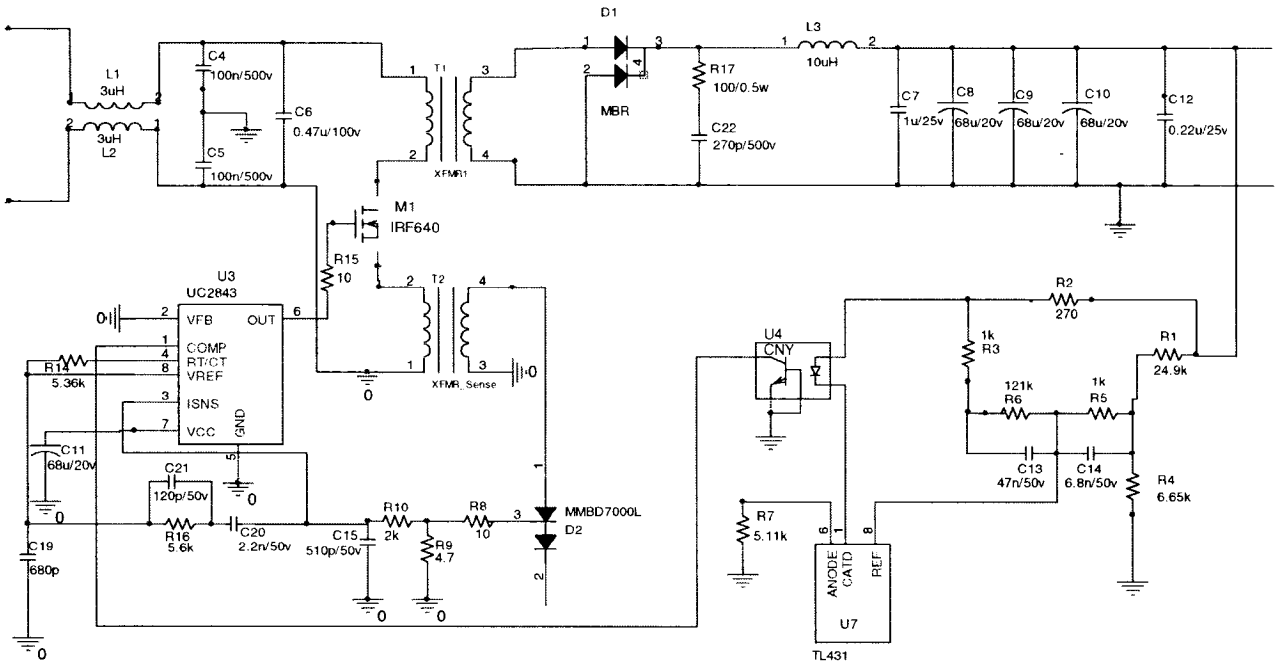

Figure B.1 Schematic Diagram of the DC/DC Converter

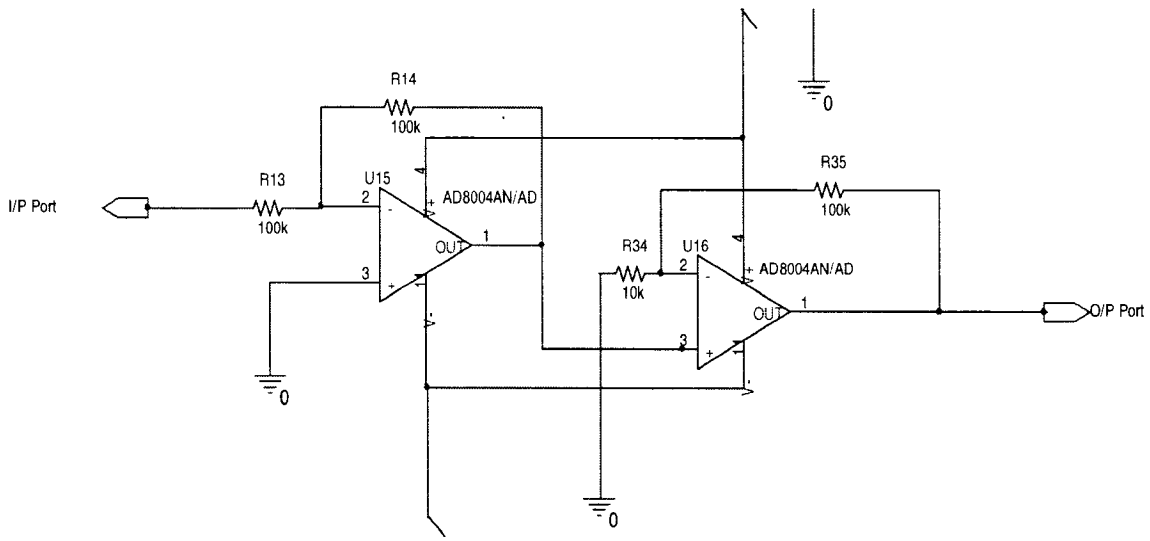

Figure B.2 Schematic diagram of Active EMI filter

Table B.1 List of Components Used in the design

Item Number	Quantity	Value	Part Reference
1	1	100n/500v	C1
2	1	100n/500v	C2
3	1	0.47u	C3
4	1	100n/500v	C4
5	1	100n/500v	C5
6	1	0.47u/100v	C6
7	1	1u/25v	C7
8	1	68u/20v	C8
9	1	68u	C9
10	1	68u	C10
11	1	68u	C11
12	1	0.22u	C12
13	1	47n	C13
14	1	6.8n	C14
15	1	510p	C15
16	1	0.22u	C16
17	1	0.68u	C17
18	1	1u	C18
19	1	680p	C19
20	1	2.2n	C20

21	1	120p	C21
22	1	270p	C22
23	1	MBR	D1
24	1	MMBD7000L	D2
25	1	MMBD7000L	D3
26	1	murs205	D4
27	1	3uH	L1
28	1	3uH	L2
29	1	IRF640	M1
30	1	24.9k	R1
31	1	270	R2
32	1	1k	R3
33	1	6.65k	R4
34	1	1k	R5
35	1	121k	R6
36	1	5.11k	R7
37	1	10	R8
38	1	4.7	R9
39	1	2k	R10
40	1	432	R11
41	1	22.1k	R12
42	1	6.87k	R13
43	1	5.36k	R14
44	1	3.3	R15
45	1	5.6k	R16
46	1	100/0.5w	R17
47	1	XFMR1	T1
48	1	XFMR_Sense	T2
49	1	UC2843	U3
50	1	CNY	U4
52	1	TL431	U7
53	1	L3/23.5uH	U8

B.2. PCB Layout

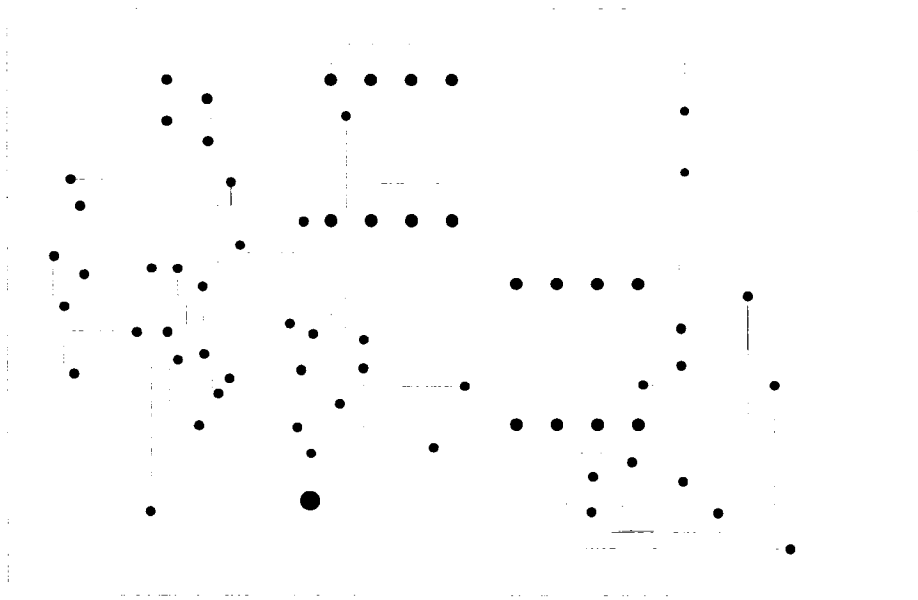

Figure B.3 DC/DC converter PCB Layout (Bottom Layer)

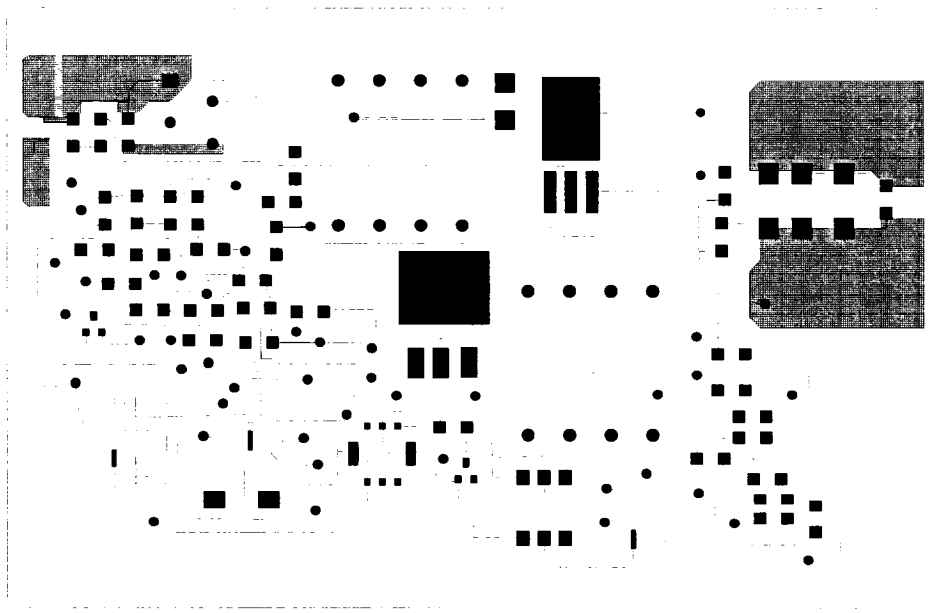

Figure B.4 DC/DC Converter PCB Layout (Top Layer)

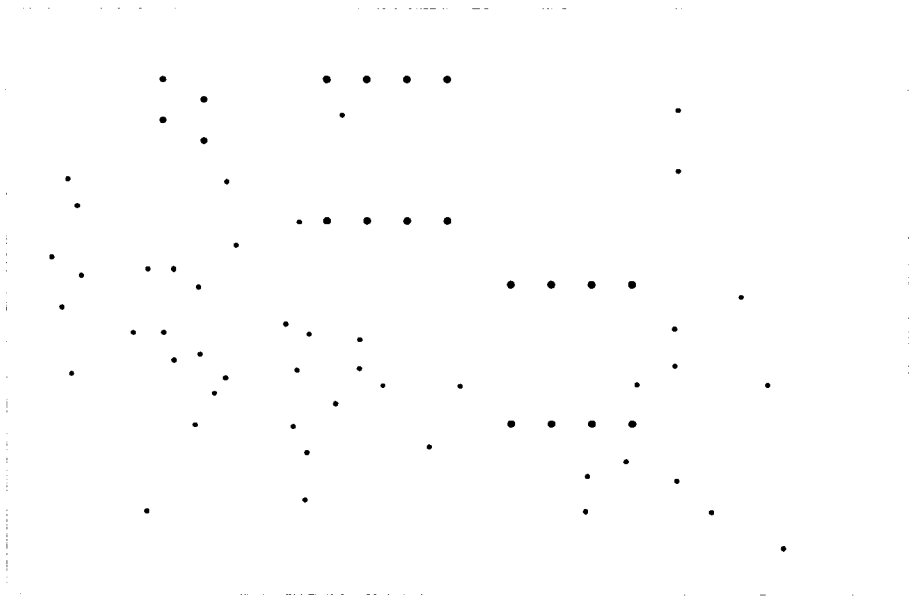

Figure B.5 DC/DC converter PCB layout (Drill layer)

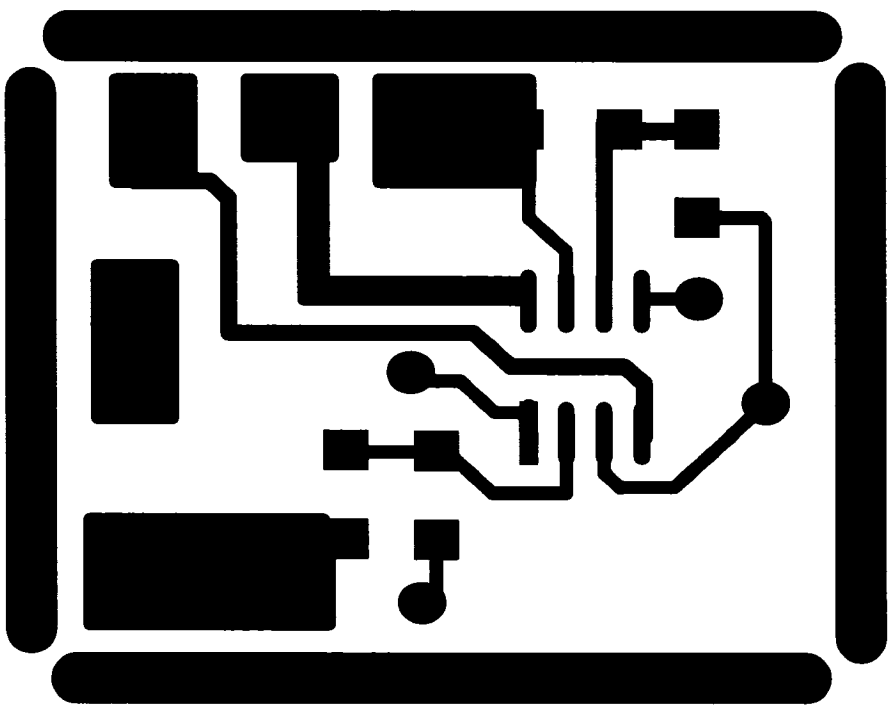

Figure B.6 Active filter PCB layout (Top layer)

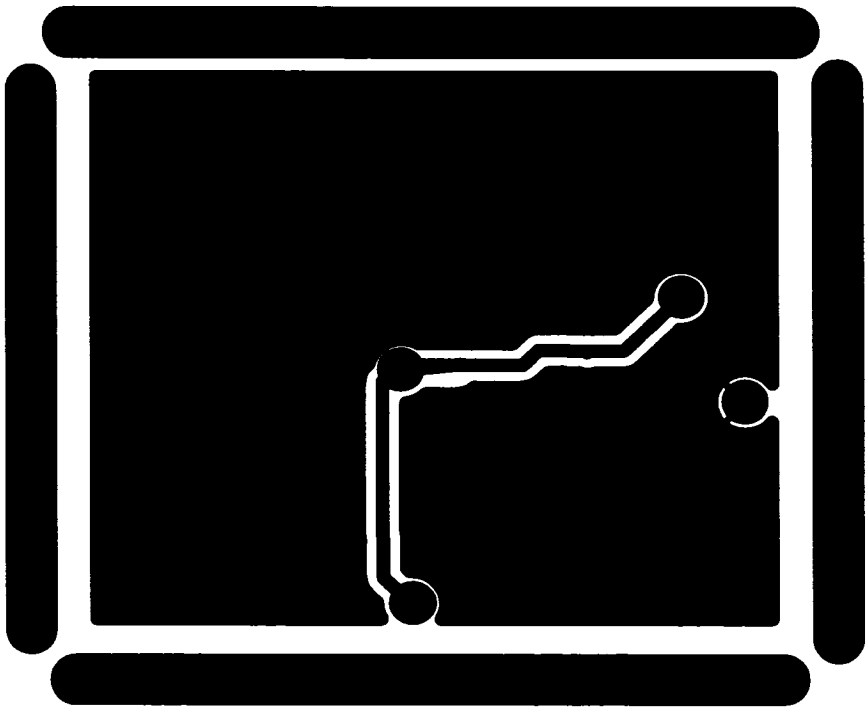

Figure B.7 Active filter PCB layout (Bottom layer)

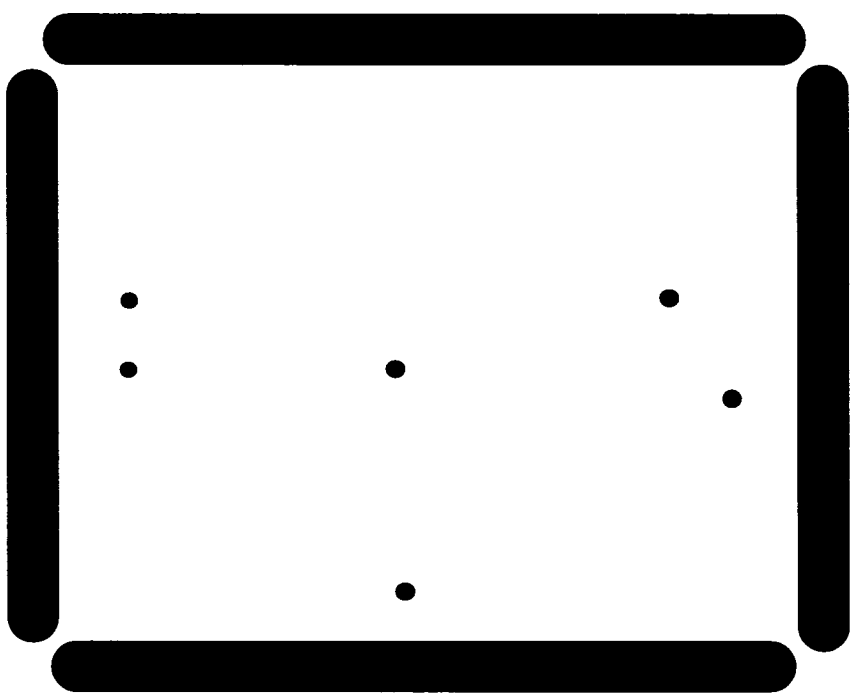

Figure B.8 Active filter PCB layout (Drill layer)

APPENDIX C

Simulation Files

This appendix contains all the simulation schematic diagram files of the entire circuit, including the active filter. It also, lists the PSPICE source code.

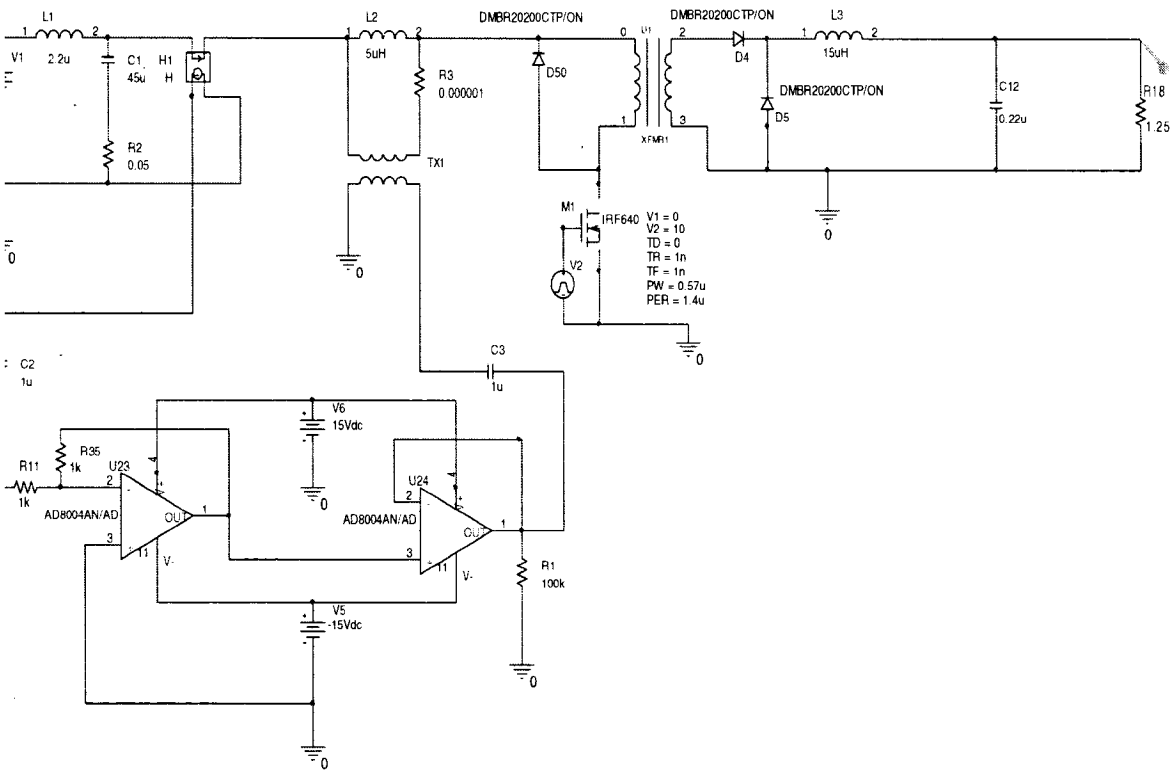

Figure C.1 DC/DC converter Simulation diagram including the active EMI filter

* PSPICE source code for the DC/DC converter including the HYBRID EMI filter

```
**********************************************************************
D_D50       N136168 N658845 DMBR20200CTP/ON
V_V6        N833831 0 15Vdc
D_D5        0 N136144 DMBR20200CTP/ON
D_D4        N183157 N136144 DMBR20200CTP/ON
R_R35       N866096 N833347  1k
L_L1        N831470 N825089  2.2u
X_U1        N658845 N136168 N183157 0 XFMR1 PARAMS:  RATIO=0.5
V_V1        N831470 0 28Vdc
L_L2        N835632 N658845  5uH
X_U24       N833347 N833343 N833831 N833291 N833343 AD8004AN/AD
L_L3        N136144 N136216  15uH
C_C1        N831286 N825089  45u
R_R18       0 N136216  1.25
X_TX1    0 N835967 N835632 N854932 SCHEMATIC1_TX1
R_R11       N835440 N866096  1k
X_U23       0 N866096 N833831 N833291 N833347 AD8004AN/AD
R_R2        0 N831286  0.05
C_C2        N835440 N835253  1u
C_C3        N835967 N833343  1u
X_H1     N825089 N835632 N835253 0 SCHEMATIC1_H1
C_C12       0 N136216  0.22u
R_R3        N854932 N658845  0.000001
V_V5        N833291 0 -15Vdc
M_M1        N136168 N136908 0 0 IRF640
V_V2        N136908 0
+PULSE 0 10 0 1n 1n 0.57u 1.4u
R_R1        0 N833343  100k
**************************************
* Injection transformer
**************************************
.subckt SCHEMATIC1_TX1 1 2 3 4
K_TX1       L1_TX1 L2_TX1 1
L1_TX1       1 2 0.5uH
L2_TX1       3 4 1uH
.ends SCHEMATIC1_TX1
**************************************
* Current Controlled voltage source (CCVS)
**************************************
.subckt SCHEMATIC1_H1 1 2 3 4
H_H1        3 4 VH_H1 0.1
VH_H1        1 2 0V
```